

# The 2014 Eruptions of Pavlof Volcano, Alaska



Scientific Investigations Report 2017–5129

**Cover.** Photograph showing north flank of Pavlof Volcano, July 22, 2017. Photograph taken by Chris Waythomas, U.S. Geological Survey, Alaska Volcano Observatory.

# **The 2014 Eruptions of Pavlof Volcano, Alaska**

By Christopher F. Waythomas, Matthew M. Haney, Kristi L. Wallace, Cheryl E. Cameron, and David J. Schneider

Scientific Investigations Report 2017–5129

**U.S. Department of the Interior**  
**U.S. Geological Survey**

**U.S. Department of the Interior**

RYAN K. ZINKE, Secretary

**U.S. Geological Survey**

William H. Werkheiser, Deputy Director  
exercising the authority of the Director

U.S. Geological Survey, Reston, Virginia: 2017

For more information on the USGS—the Federal source for science about the Earth, its natural and living resources, natural hazards, and the environment—visit <https://www.usgs.gov> or call 1–888–ASK–USGS.

For an overview of USGS information products, including maps, imagery, and publications, visit <https://store.usgs.gov>.

Any use of trade, firm, or product names is for descriptive purposes only and does not imply endorsement by the U.S. Government.

Although this information product, for the most part, is in the public domain, it also may contain copyrighted materials as noted in the text. Permission to reproduce copyrighted items must be secured from the copyright owner.

Suggested citation:

Waythomas, C.F., Haney, M.M., Wallace, K.L., Cameron, C.E., and Schneider, D.J., 2017, The 2014 eruptions of Pavlof Volcano, Alaska: U.S. Geological Survey Scientific Investigations Report 2017-5129, 27 p., <https://doi.org/10.3133/sir20175129>.

ISSN 2328-0328 (online)

## Acknowledgments

We thank the many individuals not listed as authors who contributed to the monitoring and analysis of the 2014 Pavlof eruptions. Pilots and local observers in Cold Bay, Sand Point, and King Cove provided information and photographs of the volcano, which were invaluable to the Alaska Volcano Observatory staff and assisted greatly in our evaluation of the eruptive activity. Leslie Hayden, USGS, provided microprobe analyses of volcanic glass from Pavlof tephra. The senior author thanks Alex Iezzi in particular for her able field assistance and analysis of flowage signals in the seismic data.

## Contents

Introduction .....	1
Chronology of 2014 Eruptions .....	1
May 30, 2014.....	1
May 31, 2014.....	3
June 1, 2014.....	3
June 2–4, 2014 .....	3
June 5, 2014.....	7
June 6–29, 2014 .....	8
November 12, 2014.....	8
November 13–15, 2014 .....	9
November 16–26, 2014 .....	10
Eruptive Products.....	10
Lava Flows.....	12
Hot Granular Rock Avalanches.....	13
Lahars.....	14
Tephra.....	17
Impacts.....	18
Discussion and Summary.....	19
References Cited.....	26

## Appendixes

[Available for download at <https://doi.org/10.3133/sir20175129>]

1. Chemical data for The 2014 Eruptions of Pavlof Volcano.
- 2a. Major-oxide glass geochemistry for historical Pavlof tephra fall deposits.
- 2b. Point and normalized major-element glass compositions from select tephra falls from Pavlof volcano, determined by electron probe microanalyzer at the U.S. Geological Survey in Menlo Park, California.

## Figures

1. Line map showing location of Pavlof Volcano and other locations.....2
2. Oblique aerial photograph of the initial 2014 eruption plume issuing from the north flank of Pavlof Volcano, 03:43 UTC June 1 (19:43 AKDT May 31).....3
3. Seismic data showing low-level pulsatory tremor and lahar signals .....
4. Mid-infrared National Oceanic and Atmospheric Administration (NOAA) -18 satellite image showing strong thermal signals at the summit of Pavlof Volcano, 7:30 AKDT, June 2, 2014 (15:35 UTC).....5
5. Satellite image showing sulfur dioxide plume near Pavlof Volcano, June 3, 2014 .....
6. Plot of real-time seismic amplitude (RSAM) from station PV6 for the May-June eruptive period, includes significant observations and events May 30–June 6, 2014.....6
7. Photograph showing lava fountaining and incandescent mass flow at Pavlof Volcano during the early morning on June 3, 2014.....7

8.	Photograph of Pavlof Volcano on June 2, 2014, as observed from Cold Bay, Alaska .....	7
9.	Ozone Monitoring Instrument (OMI) satellite data showing sulfur dioxide plume from Pavlof Volcano, June 5, 2014.....	7
10.	Real-time seismic amplitude (RSAM) plot from station PS4A for the period November 12–28, 2014 showing increase in seismicity and other noteworthy events that occurred during this brief eruptive period .....	8
11.	Photograph showing low-level ash emission and lava fountaining at Pavlof Volcano as observed from Cold Bay, Alaska 17:30 AKST, November 12, 2014 (02:30 UTC, November 13) ..	9
12.	Image from Moderate Resolution Imaging Spectroradiometer (MODIS) visible data showing ash plume from Pavlof Volcano 13:19 AKST, (22:19 UTC) November 13, 2014 .....	9
13.	Image from Moderate Resolution Imaging Spectroradiometer (MODIS) visible data showing ash plume from Pavlof Volcano 14:30 AKST (23:00 UTC), November 15, 2014.....	10
14.	Map of Infrared Atmospheric Sounding Interferometer (IASI) satellite data showing sulfur dioxide plume generated by the eruptive activity of November 15, 2014.....	11
15.	Photograph showing minor ash emission on north flank of Pavlof Volcano caused by collapse of unstable and still cooling accumulation of spatter generated by eruptive activity in November, 2014.....	11
16.	Map of principal eruptive products associated with the 2014 eruptions of Pavlof Volcano ...	12
17.	Photographs showing spatter-fed lava flows from the November 2014 eruption of Pavlof Volcano .....	13
18.	Alkali versus silica diagram showing compositional variation of Pavlof lava flows .....	13
19.	Photograph showing scoriaceous granular rock avalanche deposits on north flank of Pavlof Volcano .....	14
20.	Graph of approximate duration of flowage (lahar) signals and time of onset at seismic station PV6 on north flank of Pavlof Volcano for lahars emplaced in June 2014 .....	15
21.	Graph of approximate duration of flowage (lahar) signals and time of onset at station PV6, north flank of Pavlof Volcano for lahars emplaced in November 2014 .....	15
22.	Photographs showing lahars on Pavlof Volcano from 2014 eruptive activity.....	16
23.	Map showing tephra deposits and approximate transit paths of significant ash clouds associated with the 2014 eruptive activity .....	17
24.	Photograph showing patchy accumulations of partially reworked tephra deposits associated with the 2014 eruptive activity .....	17
25.	Photographs showing reworked scoriaceous lapilli lag on the surface near seismic station PN7A.....	18
26.	Total alkali versus silica plot for glass analyses of representative samples of tephra from recent historical Pavlof eruptions .....	19
27.	Graph of Pavlof Volcano eruption duration in days versus eruption start date .....	20
28.	Frequency histogram of Pavlof Volcano eruption duration, 1973–2016 .....	20
29.	Graph of length of preceding repose period and eruption duration at Pavlof Volcano, 1973–2016.....	21

## Tables

1.	Comparison of Pavlof Volcano eruptions, 1973–2016 .....	22
2.	Reports of ash fall on communities near Pavlof Volcano, 1846–2016.....	25

## Abbreviations

AIRS	Atmospheric Infrared Sounder
AKDT	Alaska Daylight Time
AKST	Alaska Standard Time
ASL	Above Sea Level
AVO	Alaska Volcano Observatory
DU	Dobson Units
FAA	Federal Aviation Administration
GOME2	Second Global Ozone Monitoring Experiment
IASI	Infrared Atmospheric Sounding Interferometer
MODIS	Moderate Resolution Imaging Spectroradiometer
NOAA	National Oceanic and Atmospheric Administration
OMI	Ozone Monitoring Instrument
RSAM	Real-time seismic amplitude
USGS	U.S. Geological Survey
UTC	Coordinated Universal Time
WWLLN	World Wide Lightning Location Network

# The 2014 Eruptions of Pavlof Volcano, Alaska

By Christopher F. Waythomas, Matthew M. Haney, Kristi L. Wallace, Cheryl E. Cameron, and David J. Schneider

## Introduction

Pavlof Volcano is one of the most frequently active volcanoes in the Aleutian Island arc, having erupted more than 40 times since observations were first recorded in the early 1800s (<http://www.avo.alaska.edu/volcanoes/volcinfo.php?volname=Pavlof>). The volcano is located on the Alaska Peninsula (lat 55.4173° N, long 161.8937° W), near Izembek National Wildlife Refuge (fig. 1). The towns and villages closest to the volcano are Cold Bay, Nelson Lagoon, Sand Point, and King Cove, which are all within 90 kilometers (km) of the volcano (fig. 1). Pavlof is a symmetrically shaped stratocone that is 2,518 meters (m) high, and has about 2,300 m of relief. The volcano supports a cover of glacial ice and perennial snow roughly 2 to 4 cubic kilometers (km<sup>3</sup>) in volume, which is mantled by variable amounts of tephra fall, rockfall debris, and pyroclastic-flow deposits produced during historical eruptions. Typical Pavlof eruptions are characterized by moderate amounts of ash emission, lava fountaining, spatter-fed lava flows, explosions, and the accumulation of unstable mounds of spatter on the upper flanks of the volcano (McNutt, 1987; Waythomas and others, 2014). The accumulation and subsequent collapse of spatter piles on the upper flanks of the volcano creates hot granular avalanches, which erode and melt snow and ice, and thereby generate watery debris-flow and hyperconcentrated-flow lahars (Waythomas and others, 2014).

Seismic instruments were first installed on Pavlof Volcano in the early 1970s, and since then eruptive episodes have been better characterized and specific processes have been documented with greater certainty (McNutt, 1987; McNutt and others, 1991). The application of remote sensing techniques, including the use of infrasound data, has also aided the study of more recent eruptions (Roach and others, 2001; DeAngelis and others, 2012; Waythomas and others, 2014; Fee and others, 2016). Although Pavlof Volcano is located in a remote part of Alaska (fig. 1), it is visible from Cold Bay, Sand Point, and Nelson Lagoon, making distal observations of eruptive activity possible, weather permitting. A busy air-travel corridor that is utilized by a numerous transcontinental and regional air carriers passes near Pavlof Volcano. The frequency of air travel across the region results in a relatively large number of airborne observations of eruptive activity. During the 2014 Pavlof eruptions, the Alaska Volcano Observatory (AVO) received observations and photographs from pilots and local observers,

which aided evaluation of the eruptive activity and the areas affected by eruptive products.

This report outlines the chronology of events associated with the 2014 eruptive activity at Pavlof Volcano, provides documentation of the style and character of the eruptive episodes, and reports briefly on the eruptive products and impacts. The principal observations are described and portrayed on maps and photographs, and the 2014 eruptive activity is compared to historical eruptions.

## Chronology of 2014 Eruptions

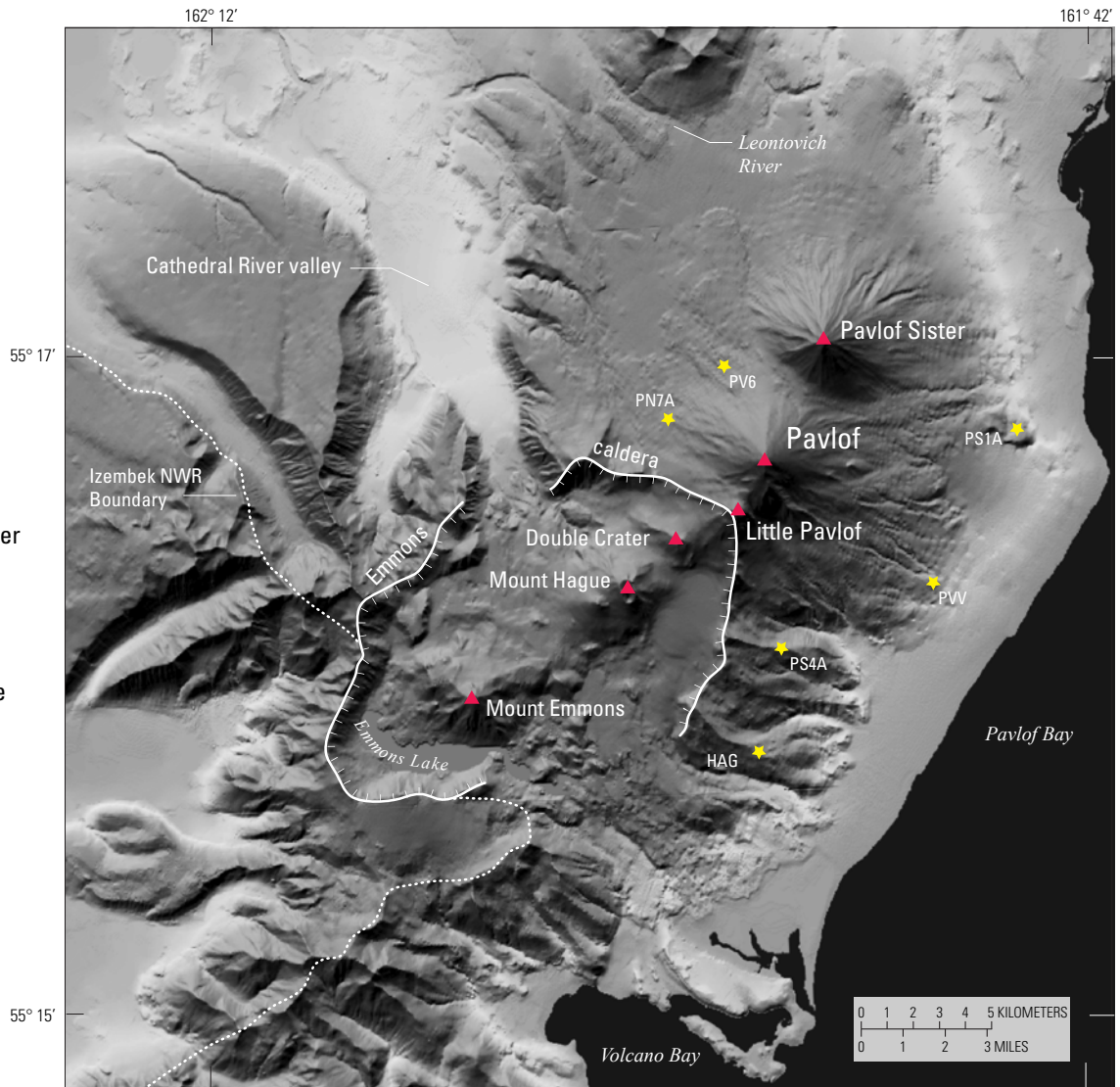
Pavlof Volcano erupted twice in 2014; during a period from May through June, and again in November (Cameron and others, 2017). During the quiescent period between the two eruptions, the volcano returned to background levels of seismicity and exhibited no detectable signs of unrest. The following narrative describes the sequence of events and observations of eruptive activity during these two 2014 eruptive episodes.

### May 30, 2014

The first of the two eruptions of Pavlof Volcano in 2014 began on May 30 and was confirmed by the appearance of a strong thermal signal identified in a satellite image acquired at 07:22 Coordinated Universal Time (UTC) May 31, 2014 (23:22 Alaska Daylight Time (AKDT) May 30). A pulsating tremor-like signal was identified retrospectively in seismic data at about 19:00 UTC (11:00 AKDT) May 30 and, though subtle, the tremor was visible on all Pavlof seismic network stations (fig. 1). Retrospective analysis of infrasound data (D. Fee, written commun., 2014) indicated that the opening phase of the eruption was detected on an infrasound network on Akutan Island about 278 km southwest of Pavlof (fig. 1). The infrasound signal began at about 07:00 UTC, May 31 (23:00 AKDT, May 30), although the signal was partially obscured by wind noise. The initial phase of the eruption was not detected by the infrasound array in Dillingham, located about 460 km northeast of Pavlof (fig. 1).

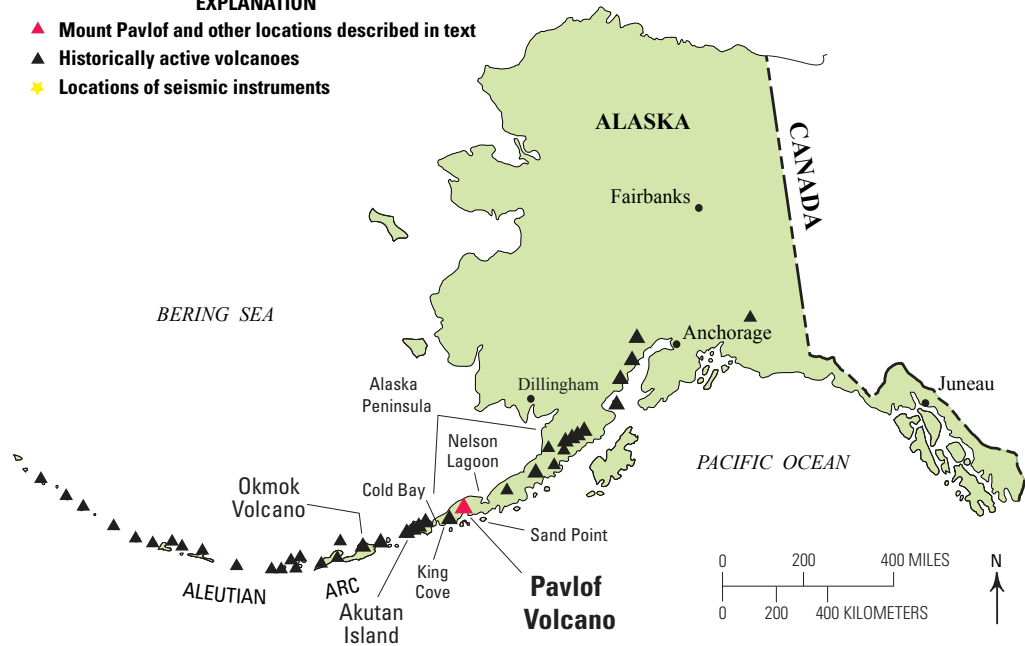
## 2 The 2014 Eruptions of Pavlof Volcano, Alaska

**Figure 1.** Line map showing location of Pavlof Volcano and other locations mentioned in text. Shaded relief map shows the locations of seismic instruments (yellow stars) that were used to detect eruptive activity at the volcano.



### EXPLANATION

- ▲ Mount Pavlof and other locations described in text
- ▲ Historically active volcanoes
- ★ Locations of seismic instruments



## May 31, 2014

As is typical of Pavlof eruptions, the tremor signal developed gradually, was barely discernable, and thus was overlooked in a routine check of seismic data that preceded the observation of a significant thermal signal at the summit. Without the intense thermal signal, which typically indicates eruptive activity in progress (Roach and others, 2001; Waythomas and others, 2014), many hours or days can pass before AVO is able to recognize that an eruption is occurring. A retrospective analysis of the seismicity on May 31 showed that there was a very slight increase in volcanic tremor for about 4 hours before eruptive activity was confirmed. By 21:09 UTC (13:09 AKDT) on May 31, the intensity of the thermal signals observed in satellite data indicated significantly elevated surface temperatures consistent with effusion of lava at the surface. AVO received the first pilot reports of ash emission from Pavlof Volcano around 03:43 UTC, June 1 (19:43 AKDT, May 31) indicating distinct ash clouds up to about 3 km above sea level (asl), just barely above the summit (2,518 m), drifting north-northeast approximately 80 km beyond the volcano (fig. 2). As a result of these observations, AVO raised the Volcano Alert Level and Aviation Color Code from GREEN/NORMAL to ORANGE/WATCH at 11:36 AKDT (19:36 UTC), May 31, 2014.

## June 1, 2014

Throughout the day of June 1, 2014 the intensity of seismic tremor remained low but detectable, and strong thermal signals were observed in satellite data.

Flowage signals were evident in seismic data (fig. 3) by late in the day on June 2 UTC (June 1, AKDT) 2014 and were detected

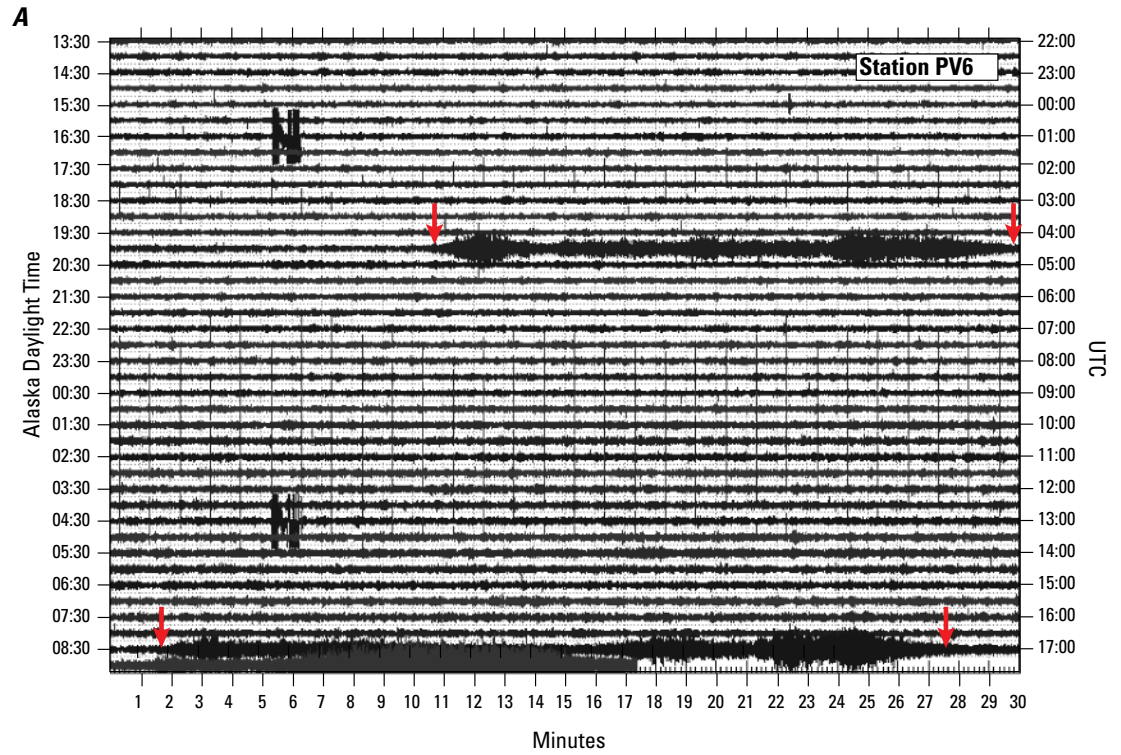
most clearly at station PV6 on the northwest flank of the volcano (fig. 1). The flowage signals appear roughly triangular-shaped in spectral plots (fig. 3A) as a result of an increase in the high frequency signal over time. In helicorder records, the flows have a characteristic elongated cigar shape (fig. 3B). Most of the flows produced signals that lasted for 15–30 minutes and were preceded by sustained low-level pulsatory tremor.

## June 2–4, 2014

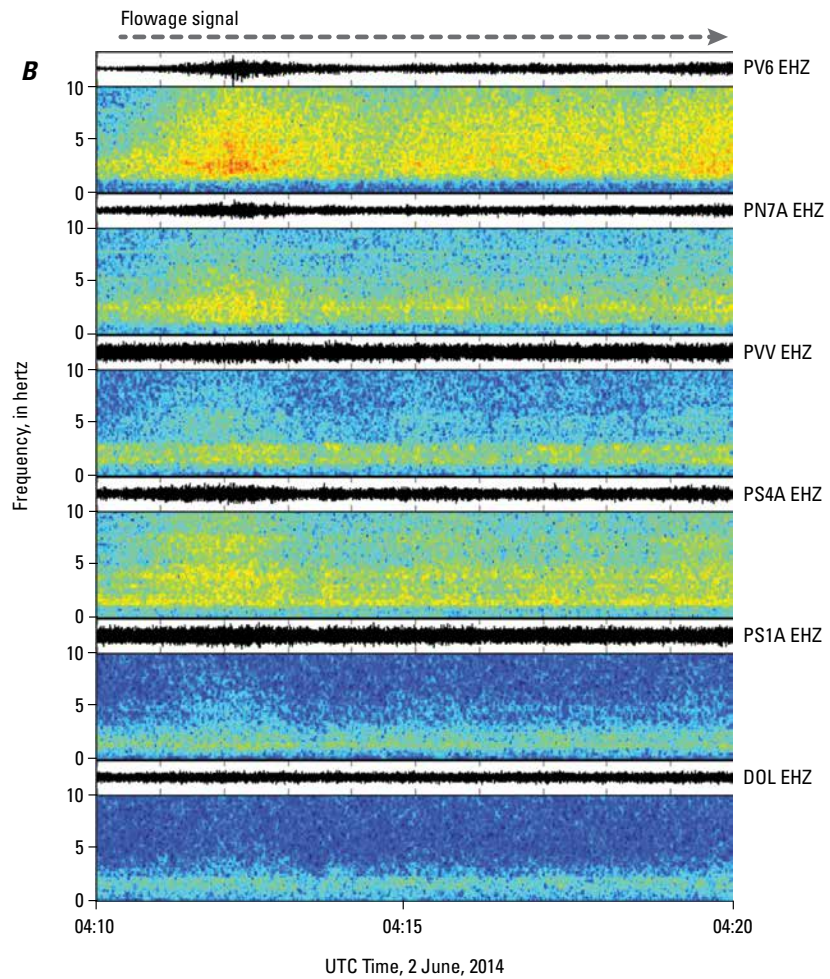
On June 2, at about 23:00 UTC (15:00 AKDT), the amplitude of the seismic tremor increased significantly; web camera views, satellite imagery, and several pilot reports indicated that a period of robust ash emission had begun. At this point, AVO raised the Volcano Alert Level and Aviation Color Code from ORANGE/WATCH to RED/WARNING, where it remained for about 24 hours. During this period, ash plumes as high as 6.7 km asl were observed by pilots in the area. During the evening hours, incandescence at the summit of the volcano was observed from Cold Bay, flowage signals continued to be detected, seismic tremor remained at high levels, and strong thermal signals were visible in satellite data (fig. 4). The ash cloud generated during this period of heightened activity extended about 100 km to the east-northeast and was observed in other satellite images extending over the community of Sand Point (fig. 1). Sulfur dioxide emissions from Pavlof Volcano were detected in satellite data from the Second Global Ozone Monitoring Experiment (GOME2) at 21:11 UTC (13:11 AKDT), June 3; maximum satellite-derived sulfur dioxide (SO<sub>2</sub>) concentrations were 11.1 Dobson units (DU) (fig. 5).



**Figure 2.** Oblique aerial photograph of the initial 2014 eruption plume issuing from the north flank of Pavlof Volcano, 03:43 UTC June 1 (19:43 AKDT May 31). The maximum plume height at the time of the photograph was roughly 3 km above sea level. Photograph by Paul Horn, Alaska Department of Fish and Game. Alaska Volcano Observatory image database url: <http://www.avo.alaska.edu/images/image.php?id=58251>.



**Figure 3.** Seismic data showing low-level pulsatory tremor and lahar signals. *A*, Helicorder record of low-level tremor and lahars during the opening phase of the 2014 eruption. Red arrows indicate approximate duration of typical lahar signals. *B*, Spectral data of low-level tremor and lahars during the same period as in *A*.



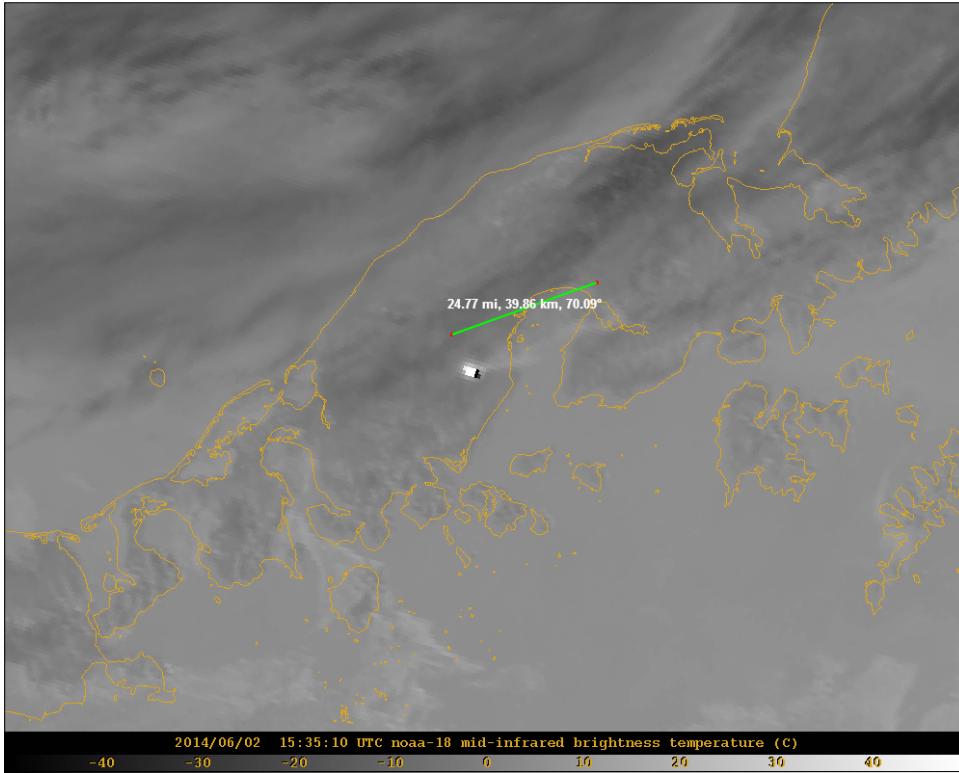


**Figure 4.** Mid-infrared National Oceanic and Atmospheric Administration (NOAA) -18 satellite image showing strong thermal signals (including black recovery pixels) at the summit of Pavlof Volcano, 7:30 AKDT, June 2, 2014 (15:35 UTC). The green scale bar indicates the approximate orientation and length of the ash plume visible in this image.

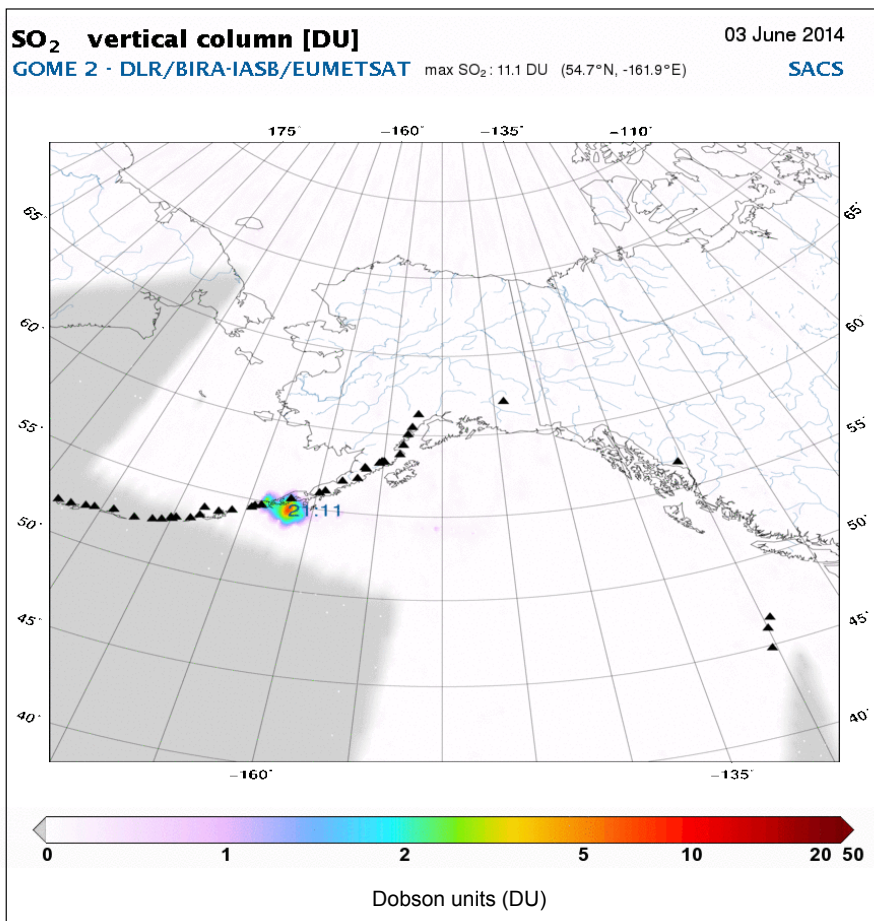


**Figure 5.** Satellite image showing sulfur dioxide plume near Pavlof Volcano, June 3, 2014. Image courtesy of Global Ozone Monitoring Experiment-2 (GOME-2).

## 6 The 2014 Eruptions of Pavlof Volcano, Alaska

From about 23:00 UTC (15:00 AKDT), June 2, until 06:30 UTC, June 3 (22:30 AKDT, June 2), the volcano was in a nearly continuous state of eruption, with sustained high levels of tremor and real-time seismic amplitude (RSAM) counts on station PS4A reaching about 600 and on station PV6 reaching about 1860 (fig. 6). Pilot reports and views from Federal Aviation Administration (FAA) weather cameras in Cold Bay indicated ash plume heights fluctuating between 6 and 7 km asl during this period.

Beginning about 06:30 UTC, June 3 (22:30 AKDT, June 2), the overall level of seismicity declined abruptly and remained elevated but fluctuating (fig. 6). At 01:54 UTC, June 4 (17:54 AKDT, June 3) AVO lowered the Aviation Color Code and Volcano Alert Level to ORANGE/WATCH in response to decreasing levels of seismic tremor. Although the tremor levels declined markedly, the level of seismic activity remained relatively steady through June 3 and 4 and was associated with several volcanic clouds, which were mostly steam and gas with minor amounts of ash, extending south of the volcano to heights of 3–9 km asl.

The activity on June 2 and 3 was characterized by episodic periods of vigorous lava fountaining (fig. 7), which resulted in the accumulation of spatter on the upper north flank of the volcano (fig. 7). Some of the spatter was of low enough viscosity to feed a lava flow. Other, higher viscosity,

spatter accumulations formed unstable piles of agglutinate that occasionally collapsed and created hot granular avalanches, which flowed rapidly down the north flank of the volcano for several kilometers (fig. 8). These events produced diffuse ash emissions and steam plumes from the lower north flank of the volcano, which resulted in areas of hazy air, with variable concentrations of ash below about 3 km asl. The ash was dispersed by low-level winds and only trace accumulations occurred around the base of the volcano. While the volcano was at Aviation Color Code and Volcano Alert Level RED/WARNING on June 2 and 3, there were no reports of significant ash fall on nearby communities. The community of Sand Point may have received trace ash fall on June 3 (UTC), but local reports are inconclusive.

A moderate level of eruptive activity continued throughout the day on June 4. Elevated surface temperatures were observed in satellite data. A visible plume, extending west about 100 km beyond the volcano and as high as 7.6 km asl, was reported by pilots and was apparent in several satellite images. Nighttime web camera images showed incandescence at the summit and SO<sub>2</sub> emissions were detected by several satellite-borne instruments (Infrared Atmospheric Sounding Interferometer (IASI), Ozone Monitoring Instrument (OMI) Atmospheric Infrared Sounder (AIRS), and Global Ozone Monitoring Experiment-2 (GOME-2)).

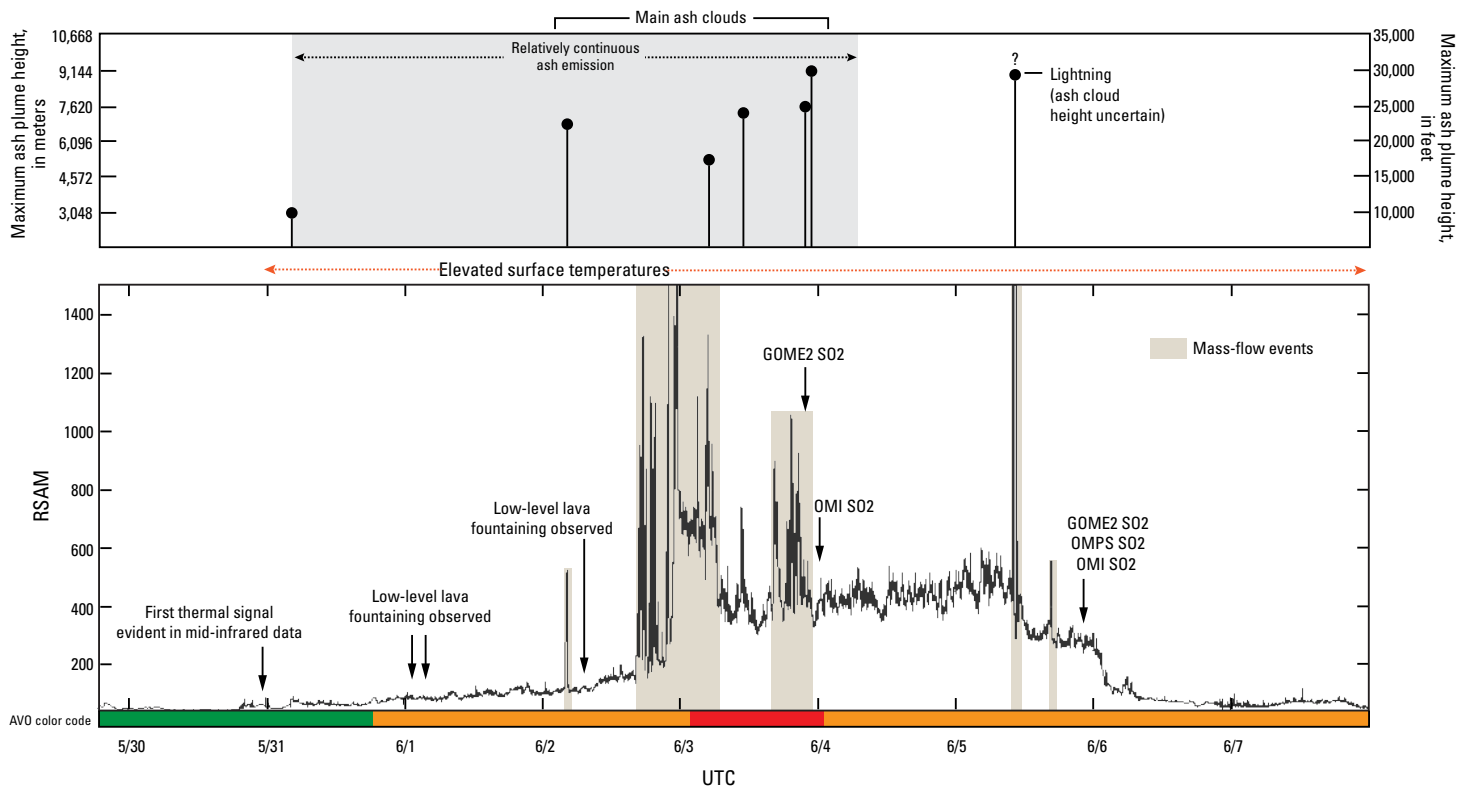


**Figure 6.** Plot of real-time seismic amplitude (RSAM) from station PV6 (fig. 1) for the May-June eruptive period, includes significant observations and events May 30–June 6, 2014.



**Figure 7.** Photograph showing lava fountaining and incandescent mass flow at Pavlof Volcano during the early morning on June 3, 2014. View from Cold Bay, Alaska, ~ 58 km (36 mi) southwest of the volcano. Photograph courtesy of Robert Stacy.



**Figure 8.** Photograph of Pavlof Volcano on June 2, 2014 (time of day unknown), as observed from Cold Bay, Alaska. The light-colored steam plume near the base of the volcano (arrow) was produced by hot granular flows mixing with snow and ice on the north flank of the volcano. The granular flows resulted from collapse of spatter accumulations emplaced near the summit vent. Photograph courtesy of Robert Stacy.

### June 5, 2014

Two periods of energetic seismicity occurred on the morning of June 5 at 10:05 and 10:45 UTC (02:05 and 02:45 AKDT). Lightning was also detected in the vicinity of Pavlof from 10:16–10:59 UTC (02:16–02:59 AKDT) on June 5 by the World Wide Lightning Location Network (WWLLN). Ash was not

apparent in satellite data at the time of these lightning reports, and meteorologic cloud tops were about 8.8 km asl. Meteorological lightning is unusual in this part of Alaska, so the lightning was likely related to volcanic ash generated by the eruptive activity at the volcano. Sulfur dioxide emissions were detected in GOME2, OMPS, and OMI satellite data on June 5, and the SO<sub>2</sub> plume extended from the volcano west-southwest about 100 km (fig. 9).

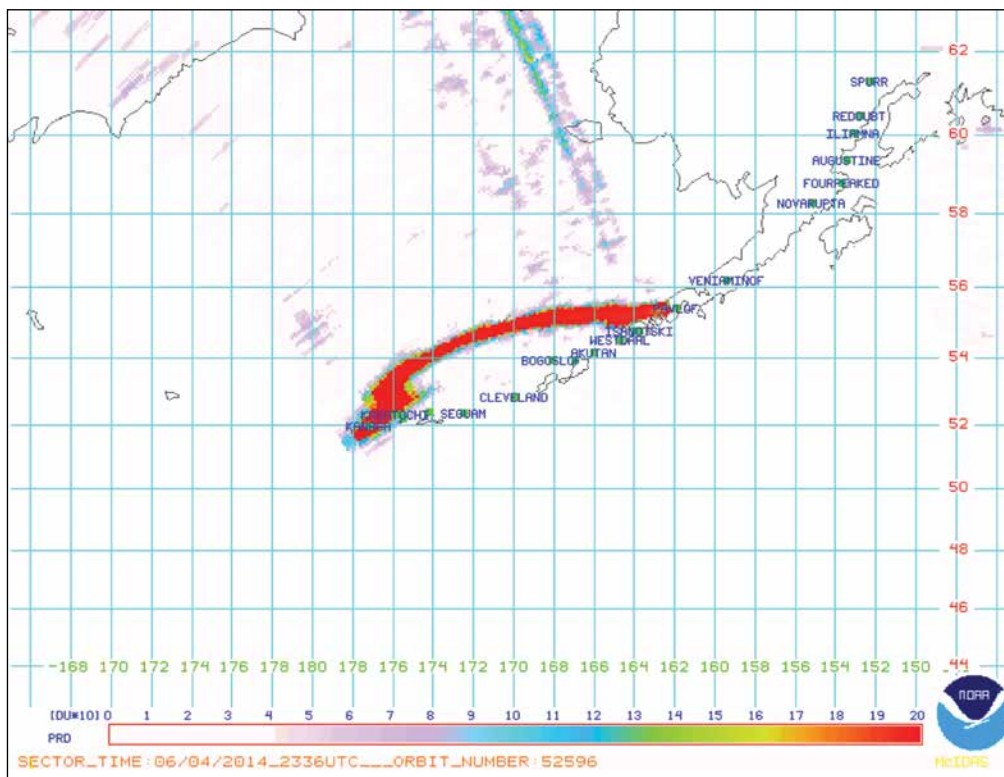


**Figure 9.** Ozone Monitoring Instrument (OMI) satellite data showing sulfur dioxide plume from Pavlof Volcano, June 5, 2014

## June 6–29, 2014

On June 6, the level of seismic activity at the volcano declined appreciably relative to the previous several days. Discrete low-frequency events, occurring at a rate of about 2 or 3 per minute, were apparent in the seismic data from stations PV6 and PN7A. Such events may have been occurring at other times during the eruption but were obscured by the sustained high levels of volcanic tremor that characterized the more robust phases of the eruption. Elevated surface temperatures at the summit of the volcano were observed in satellite data and likely indicated the continued eruption of spatter and growth of fountain-fed lava flows. Ash emissions on June 6 were greatly reduced and no ash or steam plumes were evident in satellite data over the previous 2 days, although cloud cover had obscured the volcano since then. By June 6, infrasound signals from Pavlof Volcano were no longer detected at the Dillingham or Akutan infrasound arrays indicating that significant explosive activity had ceased.

From June 6–25 the level of activity at the volcano gradually declined, discrete low-frequency events and tremors persisted for several weeks, and elevated surface temperatures became gradually weaker. Local observations indicated that low-level lava fountaining continued intermittently until about June 14, but ash emissions from June 6–14 were insignificant, confined to the upper flank of the volcano, and did not ascend much above the summit.

By about June 23, eruptive activity at Pavlof was no longer evident. Clear web camera and satellite images obtained June

23–25 revealed no evidence of lava fountaining or ash emissions. Only weakly elevated surface temperatures in the vicinity of the recently emplaced lava flows on the northeast flank were evident in satellite data. These observations resulted in the lowering of the Aviation Color Code and Volcano Alert Level to YELLOW/ADVISORY on June 25.

From June 25–July 29, unrest at the volcano continued to gradually decline. During this period there were occasional discrete low-frequency events, persistent low-level tremor that fluctuated in intensity, weakly elevated surface temperatures indicative of cooling lava and pyroclastic deposits, and occasional steam emissions from the summit vent. By July 29, the volcano had returned to its background status and the Aviation Color Code and Volcano Alert Level was reduced to GREEN/NORMAL.

## November 12, 2014

Pavlof remained quiet and at background levels of seismicity until about 0:00 UTC, November 13 (15:00 AKST, November 12), when AVO received reports of minor ash emissions and low-level lava fountaining from observers in Cold Bay. By early evening November 12, observations of low-level ash emissions several hundred meters above the volcano (about 2.7 km asl) and a sharp increase in seismic tremor (fig. 10) made it clear that Pavlof Volcano had entered a new phase of eruptive activity. As a result of these observations, AVO increased the Aviation Color Code and Volcano Alert Level to ORANGE/WATCH.

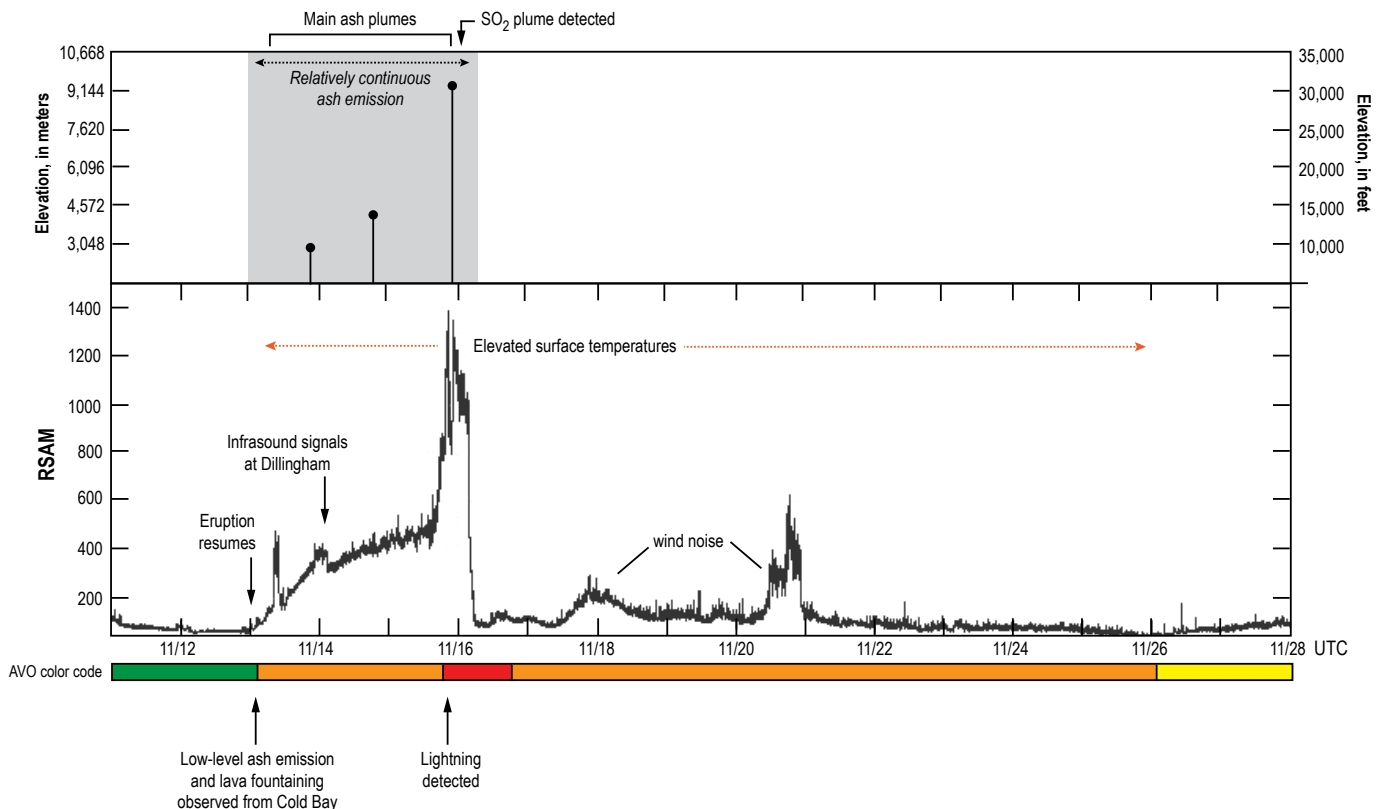


**Figure 10.** Real-time seismic amplitude (RSAM) plot from station PS4A for the period November 12–28, 2014 showing increase in seismicity and other noteworthy events that occurred during this brief eruptive period.

By late evening 12 November, highly elevated surface temperatures at the summit were observed through the clouds in a National Oceanic and Atmospheric Administration (NOAA)-18 mid-infrared satellite image, which confirmed lava at the surface and corroborated observations from Cold Bay of lava fountaining. Observers also reported flows of rock debris and ash descending the north flank of the volcano (fig. 11), and incandescence was observed in images from the Cold Bay web camera. Following the initial reports of activity on November 12, the level of seismic activity continued to increase gradually, and an intense thermal signal at the summit became persistently visible in satellite data.

### November 13–15, 2014

On 13 November, an ash plume about 200 km in length, extending northwest of the volcano, was observed in Moderate Resolution Imaging Spectroradiometer (MODIS) visible data obtained at 22:19 UTC (13:19 AKST) (fig. 12). Pilot reports from 22:30 UTC (13:30 AKST) on November 13 estimated the ash cloud top at 2.4–2.7 km asl. For the next 24 hours, seismic tremor remained at a level indicative of continuous eruptive activity, and strongly elevated surface temperatures consistent with lava fountaining were observed in satellite data. A narrow ash plume extending as far as 200 km from the volcano continued to be visible in satellite data and additional reports from pilots indicated that the ash plume eventually reached an altitude of about 4.8 km asl. Minor emissions of SO<sub>2</sub> were detected in IASI satellite data on November 14. Staff members from Izembek National Wildlife Refuge in Cold Bay reported hearing continuous rumbling sounds emanating from the volcano from about 07:00–10:30 AKST (16:00–19:30 UTC).

On November 15, the intensity of seismic tremor increased significantly over a six-hour period (fig. 10). Satellite data indicated that the ash cloud, visible for the past several days extending about



**Figure 11.** Photograph showing low-level ash emission and lava fountaining at Pavlof Volcano as observed from Cold Bay, Alaska 17:30 AKST, November 12, 2014 (02:30 UTC, November 13). Photograph by Carol Damberg, U.S. Fish and Wildlife Service. Alaska Volcano Observatory image database URL: <http://www.avo.alaska.edu/images/image.php?=-68301>.

200 km northwest of the volcano, had grown to an altitude of about 7.6 km asl. In response to this increase in eruptive activity, AVO raised the Aviation Color Code and Volcano Alert Level to RED/WARNING at 20:30 UTC (11:30 AKST) on November 15.

By 23:00 UTC (14:00 AKST), November 15, a large ash-producing eruption was clearly underway. The ash plume reached an altitude of at least 11 km asl and extended about 385 km northwest from the volcano (fig. 13). Residents of Cold Bay reported rumbling and thunder-like sounds coming from the direction of Pavlof Volcano, but were unable to make observations as the volcano was obscured by clouds. The level of infrasonic tremor detected by the infrasound array in Dillingham (fig. 1) rose steadily throughout the day

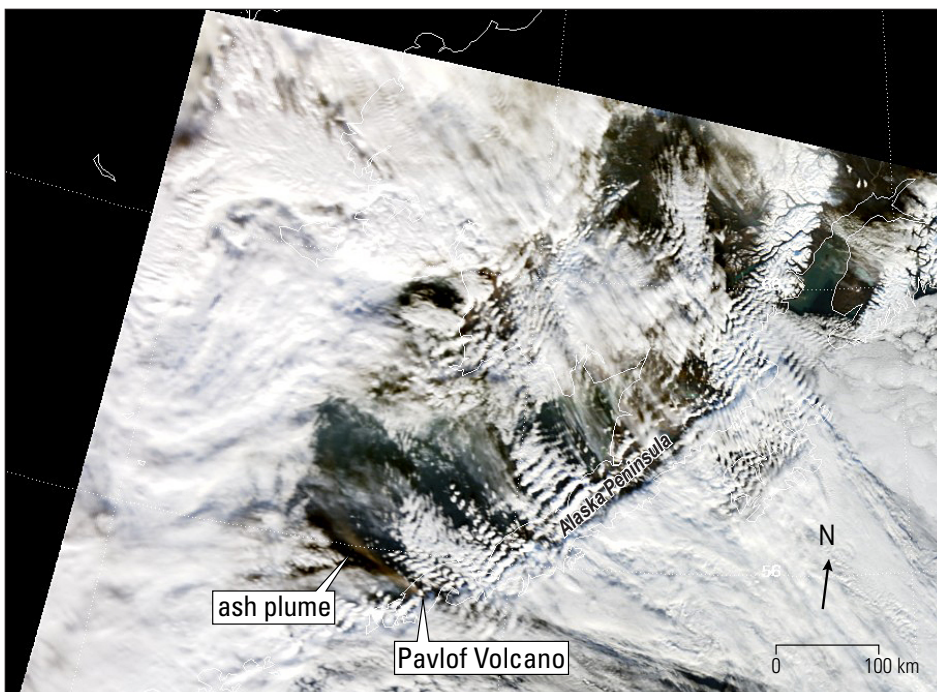


**Figure 12.** Image from Moderate Resolution Imaging Spectroradiometer (MODIS) visible data showing ash plume from Pavlof Volcano 13:19 AKST, (22:19 UTC) November 13, 2014. The plume extended ~ 200 km (124 mi) northwest of the volcano.

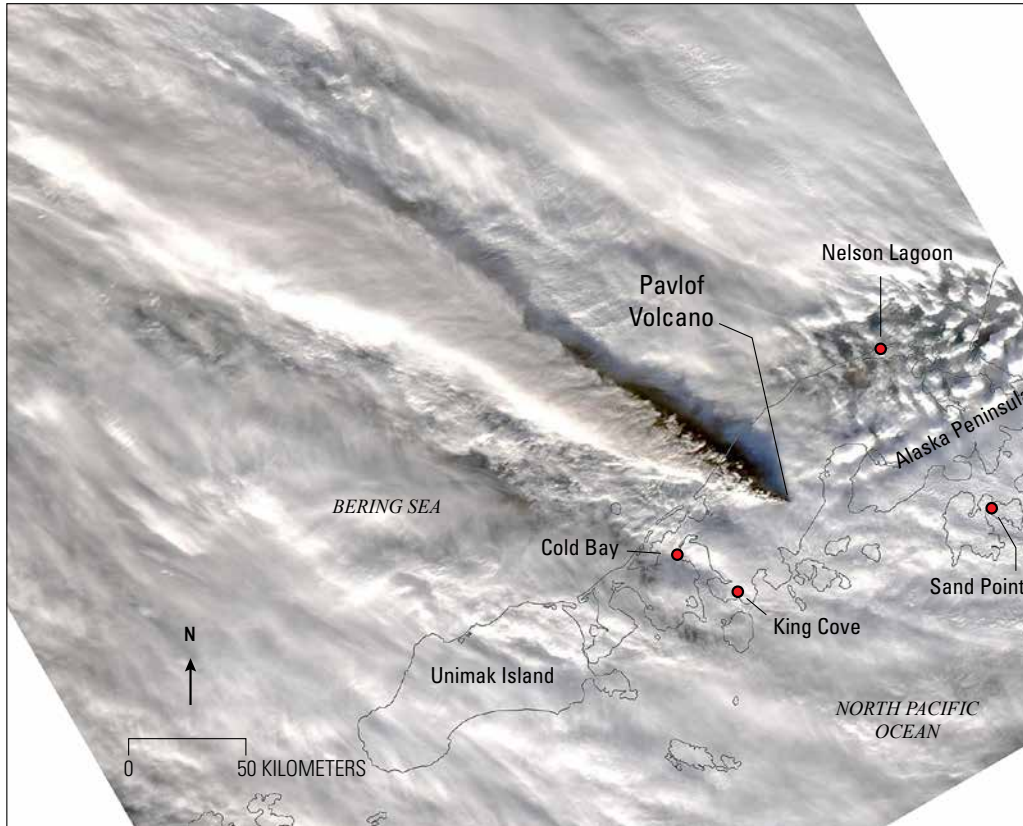


**Figure 13.** Image from Moderate Resolution Imaging Spectroradiometer (MODIS) visible data showing ash plume from Pavlof Volcano 14:30 AKST (23:00 UTC), November 15, 2014. The plume extended ~ 385 km (239 mi) northwest of the volcano.

of November 15 and reached levels slightly higher than those recorded at any time during the 2013 and May–June 2014 eruptions (D. Fee, written commun., 2014). The November 15 activity also produced an  $\text{SO}_2$  plume that was detected in IASI data at 07:35 UTC, November 16 (22:35 AKST, November 15). The  $\text{SO}_2$  plume extended westward over the Bering Strait and into Eastern Russia (fig. 14).

### November 16–26, 2014

Seismicity at the volcano decreased significantly around 04:00 UTC (19:00 AKST), November 16 and remained at low levels (fig. 10). Satellite observations confirmed a commensurate decrease in ash emissions, and ash plumes were no longer observed in satellite data after about 17:00 UTC (08:00 AKST) on November 16. In response to the decline in seismicity and ash emission, AVO lowered the Aviation Color Code and Volcano Alert Level to ORANGE/WATCH at 17:13 UTC (08:13 AKST) on November 16.

After November 16, the intensity of thermal signals at the volcano began to decline gradually. The levels of tremor fluctuated slightly, but the overall amplitude declined steadily (fig. 10) and no further seismic evidence for significant eruptive activity was observed. Satellite observations indicated that eruptive activity had

ceased about November 17. Thermal signals were occasionally observed in satellite data through about November 26, but they were the result of the still hot lava and debris on the north flank of the volcano. The low levels of seismic activity and the lack of evidence for continued lava effusion were cause for AVO to lower the Aviation Color Code and Volcano Alert Level YELLOW/ADVISORY at 00:27 UTC on November 26 (15:27 AKST, November 25).

No further eruptive activity occurred at Pavlof Volcano in 2014. Unstable accumulations of spatter continued to cool, occasionally collapsing and generating small ash emissions (fig. 15), but no further eruptive activity took place. The volcano gradually returned to normal background status and on January 15, 2015, AVO reduced the Aviation Color Code and Volcano Alert Level to GREEN/NORMAL.

### Eruptive Products

Visits to Pavlof Volcano to document and sample eruptive products were limited to two brief excursions by the senior author in August 2014 and July 2015. Descriptions and assessment of the various eruptive products generated by the 2014 eruption are thus preliminary.

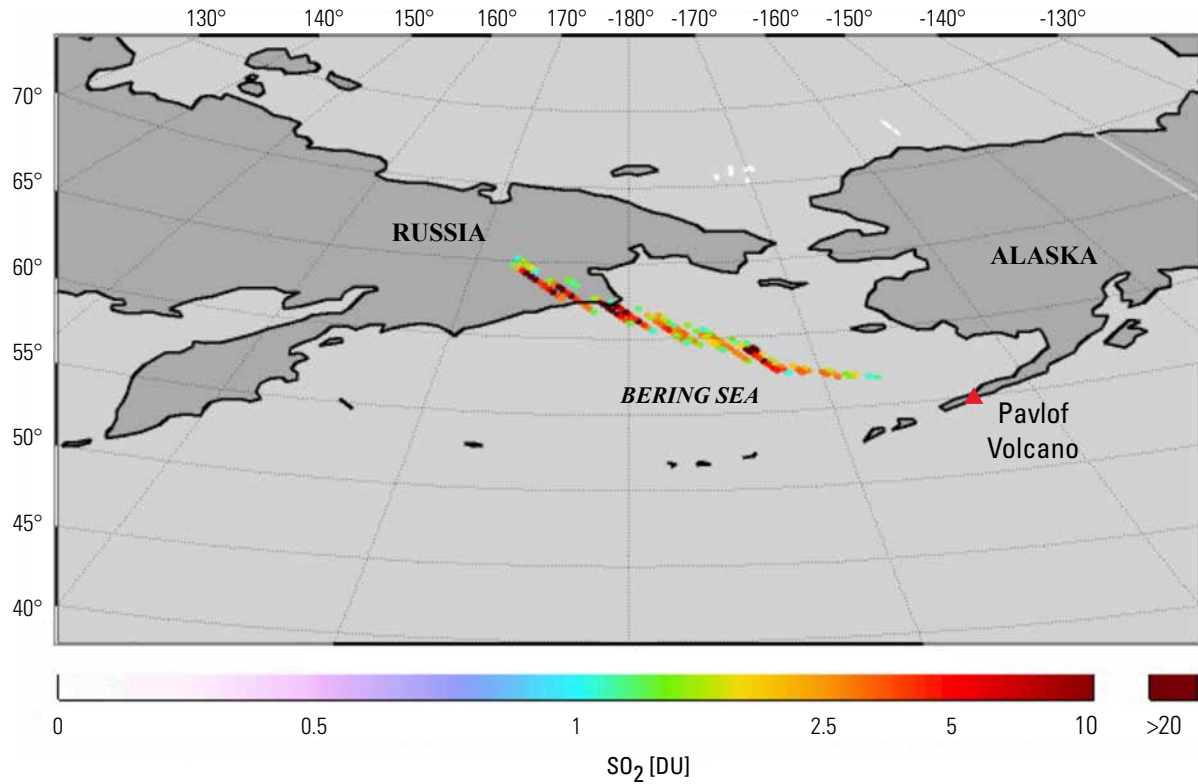


**Figure 14.** Map of Infrared Atmospheric Sounding Interferometer (IASI) satellite data showing sulfur dioxide plume generated by the eruptive activity of November 15, 2014. Sulfur dioxide values in Dobson units (DU).



**Figure 15.** Photograph showing minor ash emission on north flank of Pavlof Volcano caused by collapse of unstable and still cooling accumulation of spatter generated by eruptive activity in November, 2014. Photograph by Royce Snapp, taken November 29, 2014. Alaska Volcano Observatory image database URL: <http://www.avo.alaska.edu/images/image.php?id=68681>.

### Lava Flows

The eruptive activity in 2014 generated fountain-fed lava flows on the north flank of the volcano (fig. 16). Lava flows were generated during both the May–June and November eruptions. The May–June lava flow extended about 4.7 km from the vent and covered an area of about 0.57 square kilometers (km<sup>2</sup>). The November lava flow was slightly larger (6.3 km in length) and covered an area of about 1.13 km<sup>2</sup> extending into the lahar inundation zone of the 2014 eruption (fig. 16). Measurements of lava-flow thickness near the terminus of the November 2014 flow indicated that the lava flow in this area was 7 to 9 m thick. Using 7 m as an average thickness yields volume estimates of  $4 \times 10^6$  cubic meters (m<sup>3</sup>) for the May–June lava flow,  $8 \times 10^6$  m<sup>3</sup> for the November lava flow, and a total volume of erupted lava of  $12 \times 10^6$  m<sup>3</sup>. The 2014 lava flows were more extensive than the flows produced during the 2013 eruption, which had a volume of about  $1.5 \times 10^6$  m<sup>3</sup> (Waythomas and others, 2014).

The May–June lava flow was generated over a period of about 8 days and the average lava discharge was about 500,000 m<sup>3</sup> per day or roughly 5.8 cubic meters per second (m<sup>3</sup>/s). The November lava flow was generated over a period of 5 days and the average lava discharge was about 1,600,000 m<sup>3</sup> per day or 18.5 m<sup>3</sup>/s.

The surface morphology of the lava flows consists of narrow (1–2 km wide) lobate flows with lateral levees composed of irregular, rubbly, angular blocks and masses of dark grey to red-brown agglutinate and spatter (fig. 17). The clast-rich nature of the lava flows indicates they were derived from rapidly accumulating spatter and hot ejecta; such flows are known as clastogenic lava flows (Cas and Wright, 1988; Sumner, 1998). The flanking slopes of the lava flows have slope angles ranging from 25°–34° and include loose talus-like accumulations of boulder- to cobble-size clasts of spatter and scoriaceous material. Geochemical analysis of lava samples indicates that both the 2013 and 2014 lava flows are basaltic andesite in composition, similar to other lava flows on Pavlof Volcano (fig. 18).

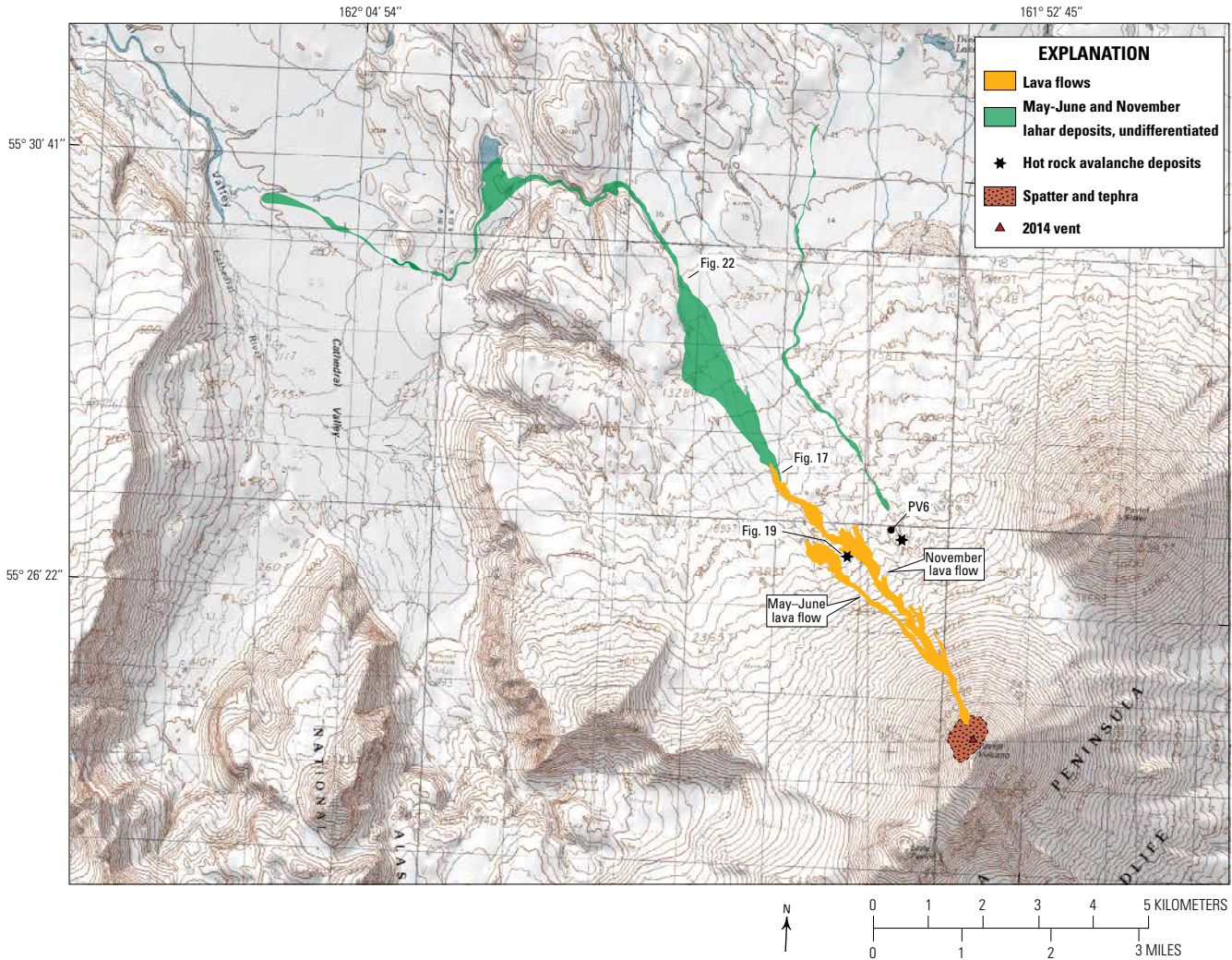


**Figure 16.** Map of principal eruptive products associated with the 2014 eruptions of Pavlof Volcano. Locations of photographs for figures 17, 19, and 22 are labeled. It was not possible to map the full extent of the hot rock avalanche deposits and the stars on the map show two locations where these deposits were identified and examined.

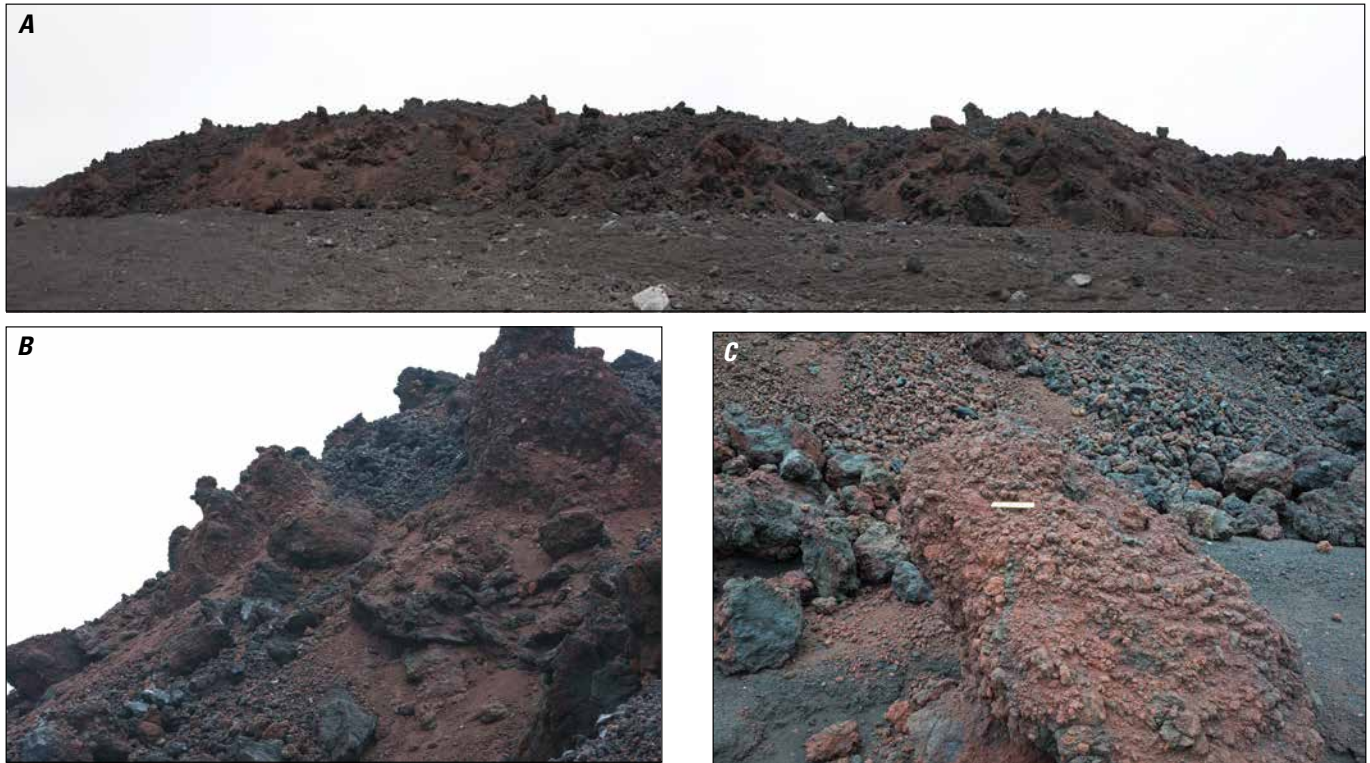


**Figure 17.** Photographs showing spatter-fed lava flows from the November 2014 eruption of Pavlof Volcano. *A*, Panorama of lava flow. Flow is 7–9 m thick at this site. *B*, Flanking slope of lava flow. Slope angles range from 25 to 34°. *C*, Typical spatter-rich lava block. Scale is 15 cm in length. See figure 16 for location of photographs.

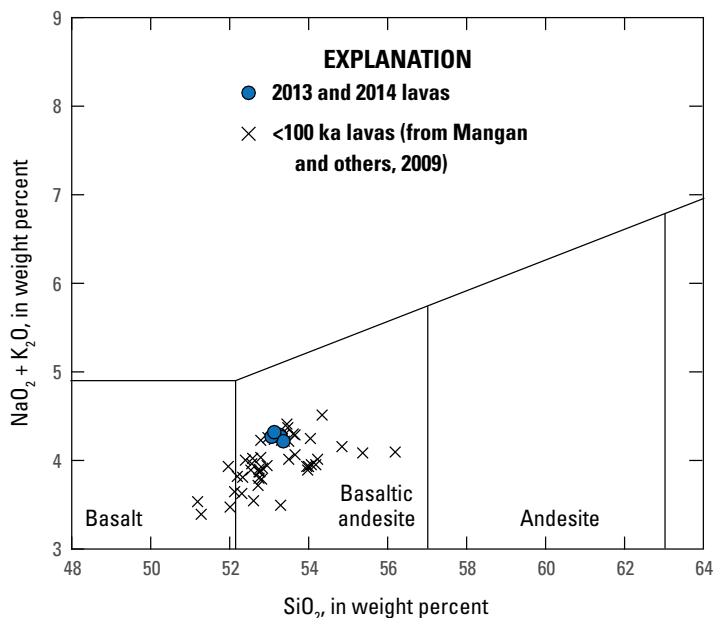


**Figure 18.** Alkali versus silica diagram showing compositional variation of Pavlof lava flows. Data on lavas <100 thousand years (ka) from Mangan and others, 2009. Data plotted for 2013 and 2014 lavas in Appendix 1.

## Hot Granular Rock Avalanches

The formation and collapse of spatter accumulations on the upper flanks of Pavlof Volcano is a characteristic process that has occurred during several historical eruptions of the volcano (Waythomas and others, 2014). Although the size, timing, and initiation mechanism for spatter-pile collapse is uncertain, a principal result of this process is the formation of hot granular flows of rock debris that sweep down the flanks of the volcano (fig. 8), sometimes flowing as far as 4–5 km from their source. The deposits of these particle-rich flows consist primarily of angular to subrounded, cobble-size clasts of rock debris that form lobe-shaped, particle-supported accumulations up to one meter thick (fig. 19). The flows are similar to pyroclastic flows but typically contain minimal amounts of fine matrix material and little to no ash. Diffuse ash plumes are sometimes associated with these hot granular flows, but the amount of ash is generally small and fine material is almost never observed in deposits on the lower flanks of the volcano (fig. 19B). The interaction of these hot granular flows with snow and ice on Pavlof Volcano is a mechanism for generating meltwater and lahars.

Fines-poor, clast-rich pyroclastic deposits developed during the August 18, and September 16 and 17, 1992 eruptions of Crater Peak (Miller and others, 1995). These deposits consist of lobate accumulations of clast-supported, dense to slightly vesiculated, cobble- to small boulder-size clasts of juvenile andesite, which

**Figure 19.** Photograph showing scoriaceous granular rock avalanche deposits on north flank of Pavlof Volcano. *A*, Lobate deposit of mostly cobble-size rock debris emplaced as a hot granular avalanche. *B*, Closeup of particles that make up granular rock avalanche deposits. Most clasts are subangular to subrounded and have a particle-supported framework that lacks fine ash matrix. See figure 16 for location of photographs.



originated chiefly by ballistic ejection of rock debris that coalesced and flowed a short distance downslope (about 3 km) as hot granular rock avalanches (Miller and others, 1995). Lava fountaining and spatter accumulation did not occur during the 1992 eruptions of Crater Peak. It remains possible that some of the hot granular mass flow deposits associated with the 2014 and other historical Pavlof eruptions may have formed in the same manner described for Crater Peak deposits of similar appearance.

## Lahars

Lahars commonly form during eruptions of Pavlof Volcano because of the ice and snow cover available for melting and the abundant supply of unconsolidated pyroclastic debris that covers much of the volcano. Meltwater to form lahars is commonly generated by the interaction of hot granular mass flows with snow and ice. The process involves a period of sustained lava fountaining and the accumulation of a sizeable mound of spatter at or just below the vent, followed by collapse of the spatter accumulation, and rapid downslope movement of a hot particulate

flow consisting of cobbles and small boulders of juvenile rock debris. These flows scour, erode, dynamically melt snow and ice, and the ensuing meltwater mixes with unconsolidated pyroclastic debris on the flank of the volcano to form a lahar. These processes are not clearly differentiated in seismic data and the flowage signals that appear in seismic records generally present as one continuous flow signal. Therefore, it is unclear which parts of the signal are attributable to hot granular mass flow and which are associated with a lahar; except that the early part of the flow signal is probably the hot granular flow and the end part of the signal is likely the lahar component.

During the 2014 eruptions, numerous flowage signals were identified in seismic data (fig. 3), primarily at station PV6 on the northwest flank of the volcano (fig. 1). The signal duration, as determined by visual analysis of the seismic data, at station PV6 allows an estimate of flow duration in the vicinity of the seismic station and is a proxy for flow magnitude. Flowage signals were detected on June 2 and 3, when eleven distinct flows were evident (fig. 20) and again on November 15 and 16, when seven flows were evident (fig. 21). During the May–June period of

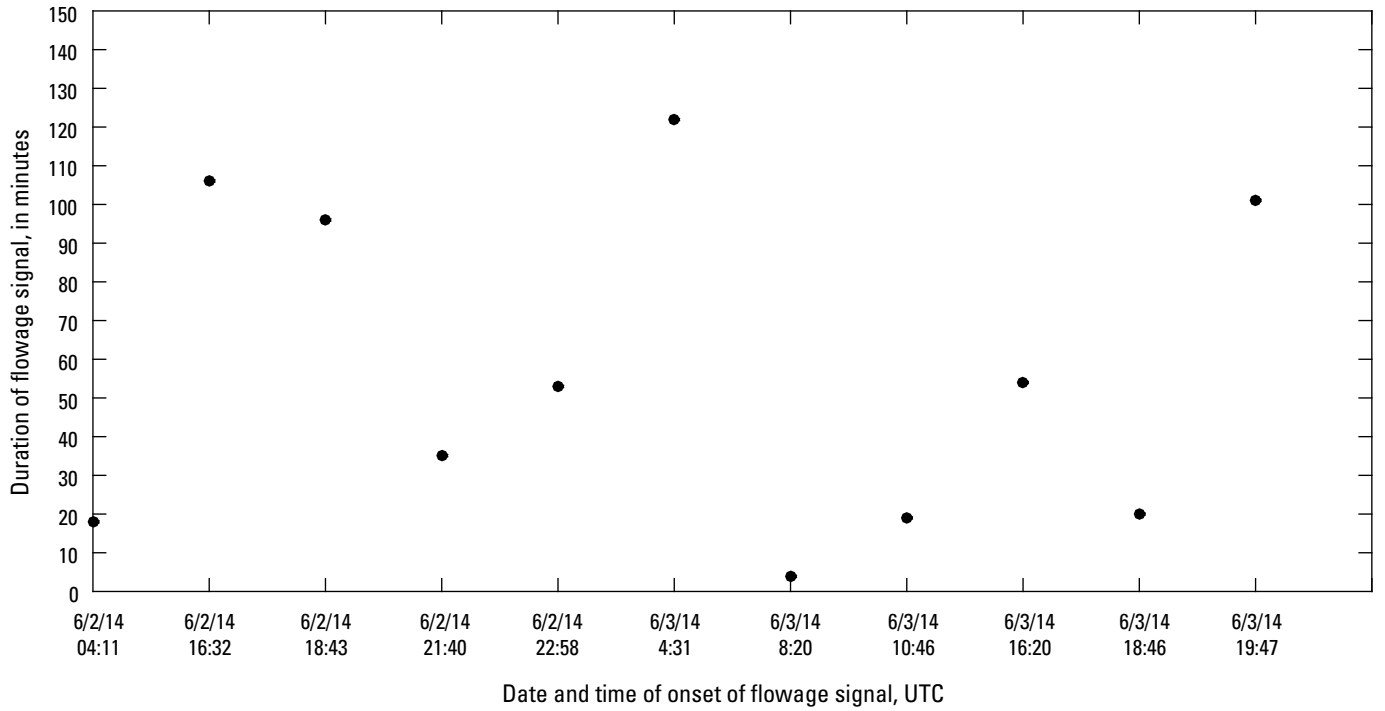


**Figure 20.** Graph of approximate duration of flowage (lahar) signals and time of onset at seismic station PV6 on north flank of Pavlof Volcano for lahars emplaced in June 2014.

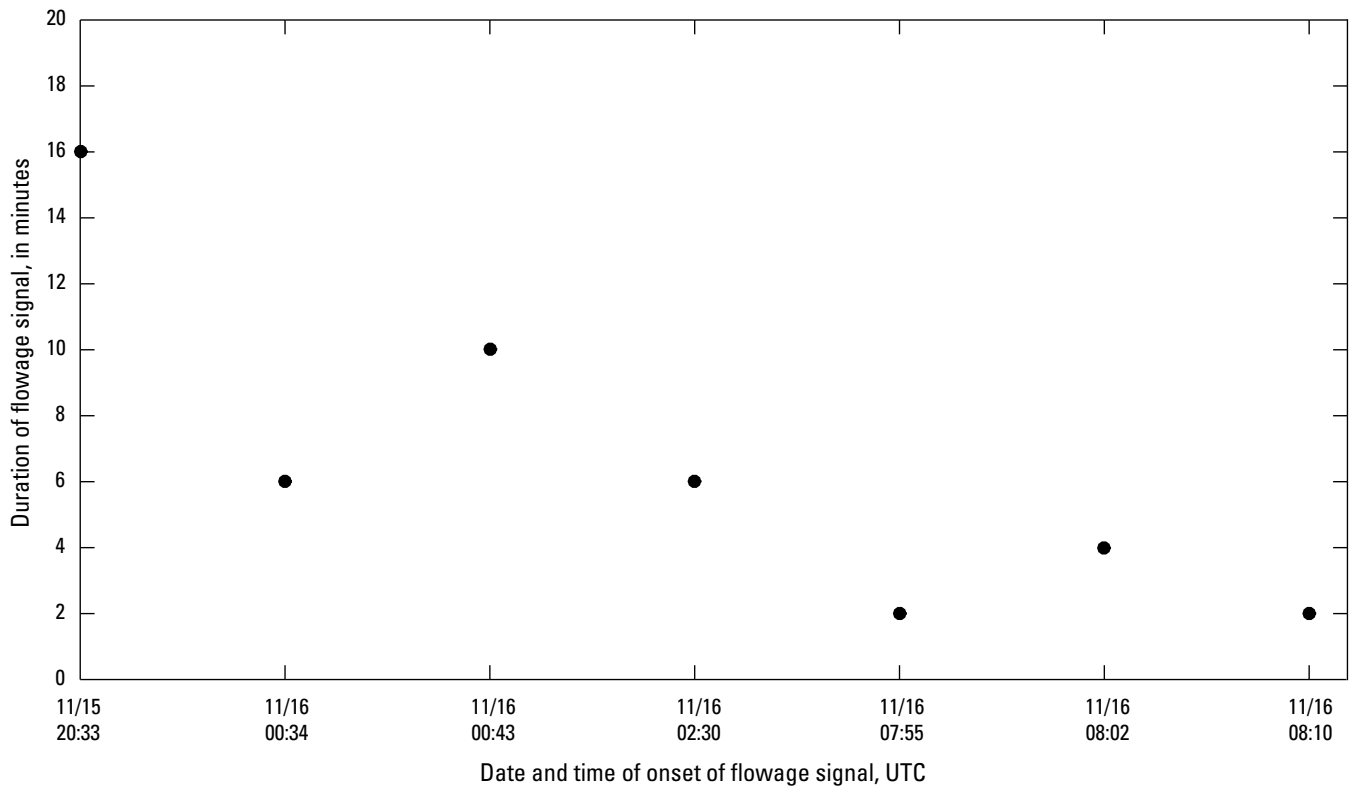


**Figure 21.** Graph of approximate duration of flowage (lahar) signals and time of onset at station PV6, north flank of Pavlof Volcano for lahars emplaced in November 2014.

## 16 The 2014 Eruptions of Pavlof Volcano, Alaska

eruptive activity, flow durations ranged from a minimum of 4 minutes to a maximum of 122 minutes, and there were four flows with signal durations >90 minutes (fig. 20). The mass flows produced during the November eruption were shorter in duration than those of the May–June eruption, all November flows had signal durations <20 minutes at station PV6 (fig. 21), whereas all but one of the May–June flows had signal durations >20 minutes (fig. 20). All of the flows occurred when the levels of seismicity were highest, indicating a general correlation of flowage signals with seismic intensity (figs. 6, 10). Although the duration of many of the flowage signals was >60 minutes, the spatial extent of lahar inundation in the drainages on the north flank of Pavlof Volcano was not particularly noteworthy

(fig. 16), suggesting that many of the flowage signals identified in seismic data were probably generated by hot granular mass flows and not water saturated lahars. The approximate area of lahar inundation resulting from the 2014 eruptions was 3.56 km<sup>2</sup> and the lahar volume was roughly 1.8–3.6 x 10<sup>6</sup> m<sup>3</sup> assuming flow depths in the range of 0.5 to 1 m.

The lahar deposits produced by the 2014 eruption consist of clast-rich, debris-flow lahar deposits and sandy, horizontally bedded, hyperconcentrated-flow lahar deposits (fig. 22). The debris-flow lahar deposits are common along channel floors, whereas the hyperconcentrated-flow deposits make up most of the distal deposits and the overbank deposits along channel margins.

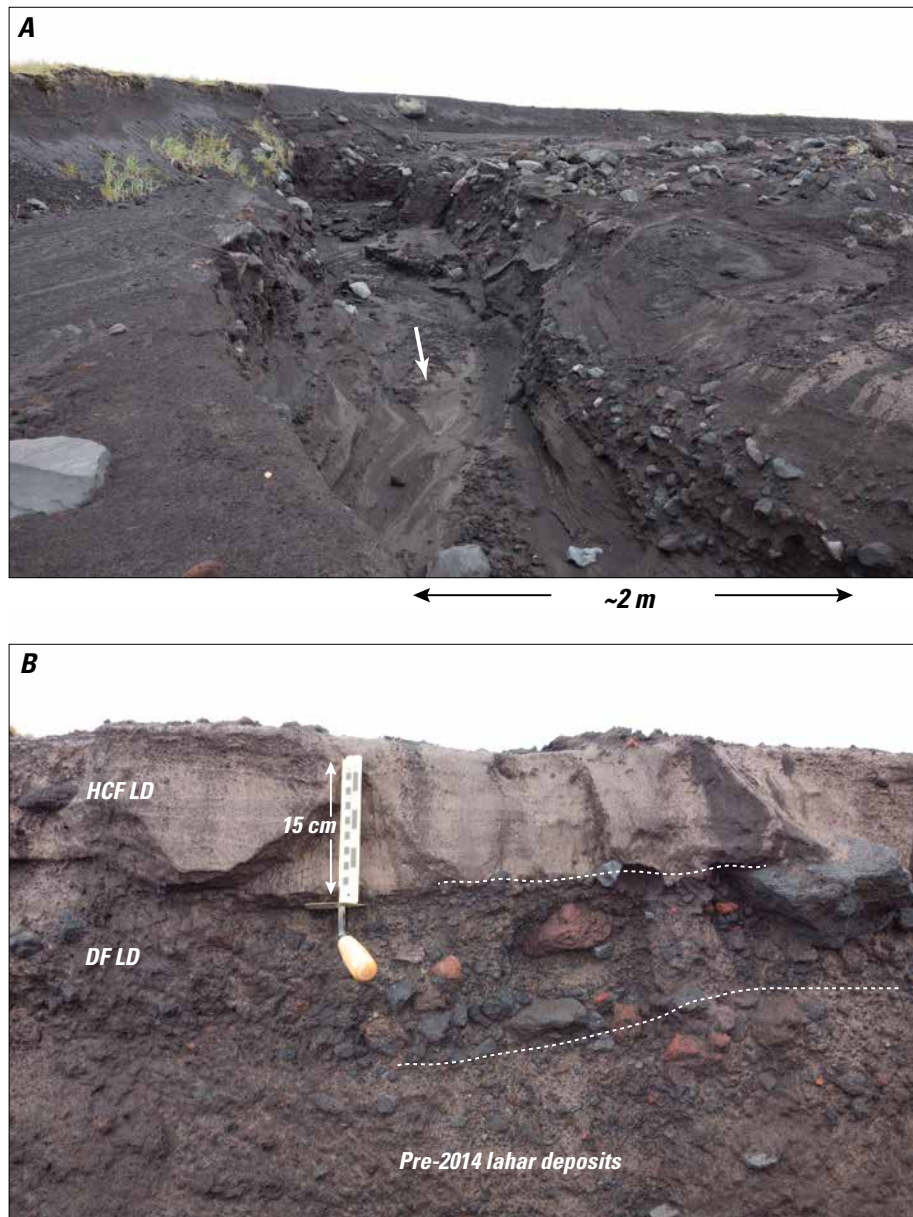


**Figure 22.** Photographs showing lahar deposits on Pavlof Volcano from 2014 eruptive activity. *A*, Typical lahar channel on northwest flank of volcano. Arrow indicates flow direction. *B*, Hyperconcentrated-flow lahar deposit (HCF LD) and debris-flow lahar deposit (DF LD) exposed in bank of lahar channel on northwest flank of Pavlof Volcano. See figure 16 for location of photographs.

### Tephra

Tephra-fall deposits were generated during the most robust phases of the 2014 eruptions of Pavlov Volcano. Measurable accumulations of tephra were limited to areas around the volcano within 10–12 km of the vent (fig. 23), but soon after deposition, many of these deposits were redistributed or partially removed

by wind. Tephra deposits could not be sampled during eruptive activity and AVO received no samples of distal tephra from any of the communities surrounding the volcano. Tephra deposits examined in August 2014 and July 2015, and presumed to have been erupted in 2014, consisted of patchy accumulations of scoriaceous lapilli, typically about 1 grain thick (5–8 cm; fig. 24), which were variously reworked by wind and thus devoid of fine

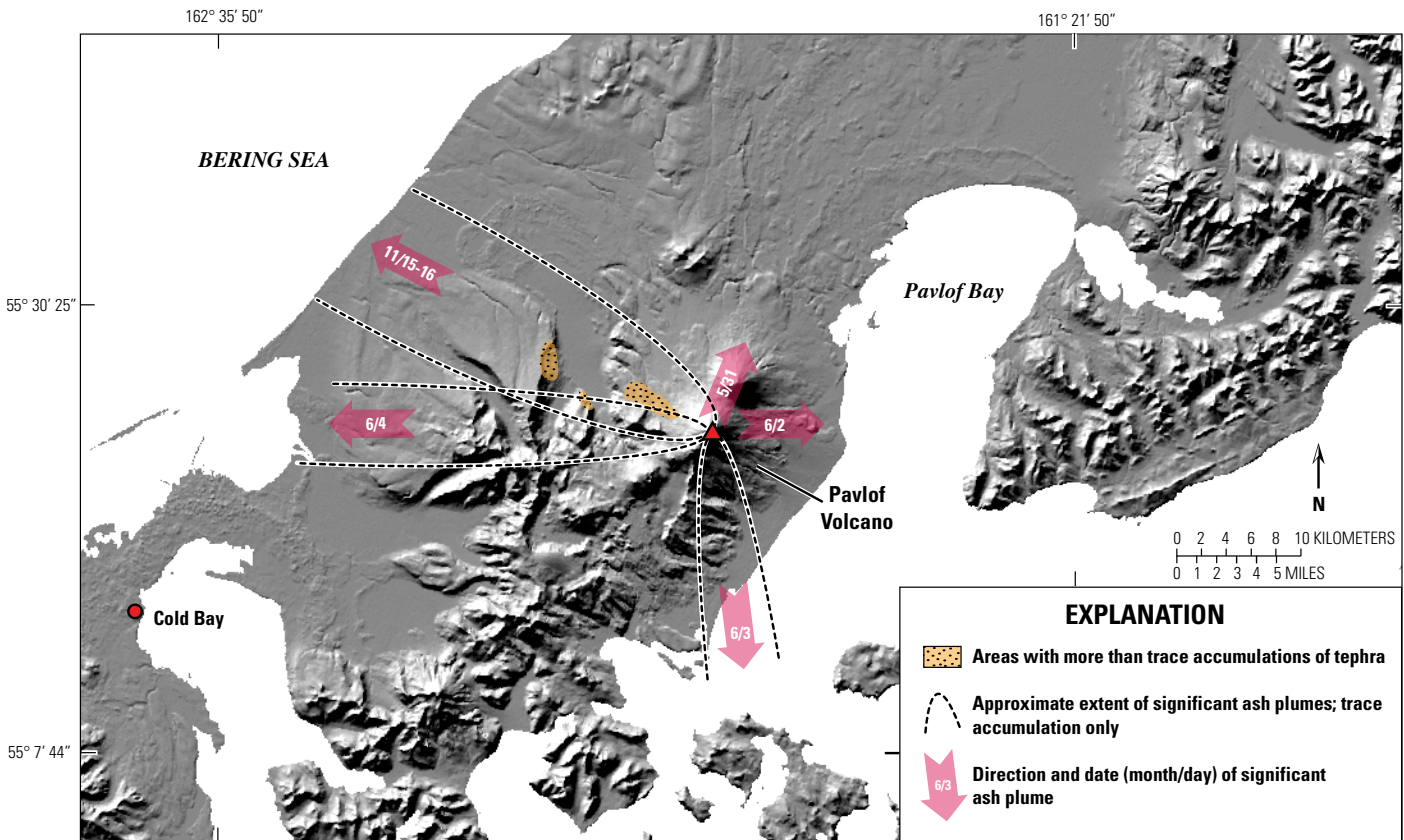


**Figure 23.** Map showing tephra deposits and approximate transit paths of significant ash clouds associated with the 2014 eruptive activity.

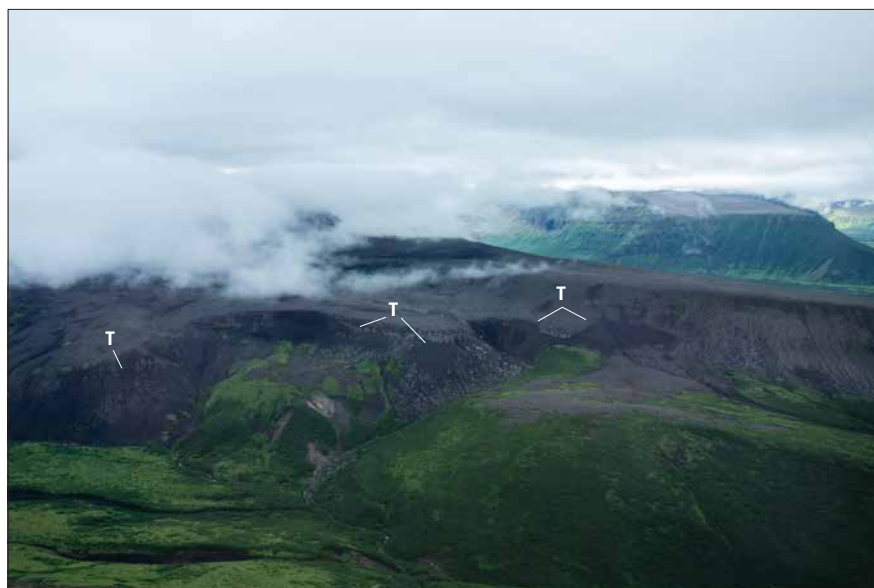


**Figure 24.** Photograph showing patchy accumulations of partially reworked tephra deposits (T) associated with the 2014 activity. The tephra deposits are about 15 km northwest of Pavlov Volcano.

ash (fig. 24). These deposits were located along major ash plume axes (fig. 23) and were not evident in summer 2013, and are thus most likely fallout from the 2014 eruption. Tephra deposits in the vicinity of seismic station PN7A, about 6 km northwest of the Pavlof summit, consisted of angular, medium- to dark-grey, scoriaceous lapilli (fig. 25) with maximum clast A-axis (long axis) dimensions as much as 8 cm. These deposits had been reworked by wind and no fine ash was present around individual lapilli. Major-oxide glass geochemical analyses of historical Pavlof tephra-fall deposits revealed that all contain glass of andesitic composition (fig. 26).

## Impacts

Pavlof Volcano is located in a remote part of Alaska and no structures or facilities close to the volcano were affected by eruptive activity, other than AVO seismic stations. Drifting ash clouds and ash fallout have the greatest effect on towns and villages in the region and occasionally interfere with air travel. Trace amounts of fine ash were reported at the Sand Point Airport (fig. 1) on June 3 and 4, which resulted in cancellation of flights to Sand Point. At least 5 flights to Cold Bay and 9 flights to Dutch Harbor were also cancelled on June 3 and 4; local commuter air

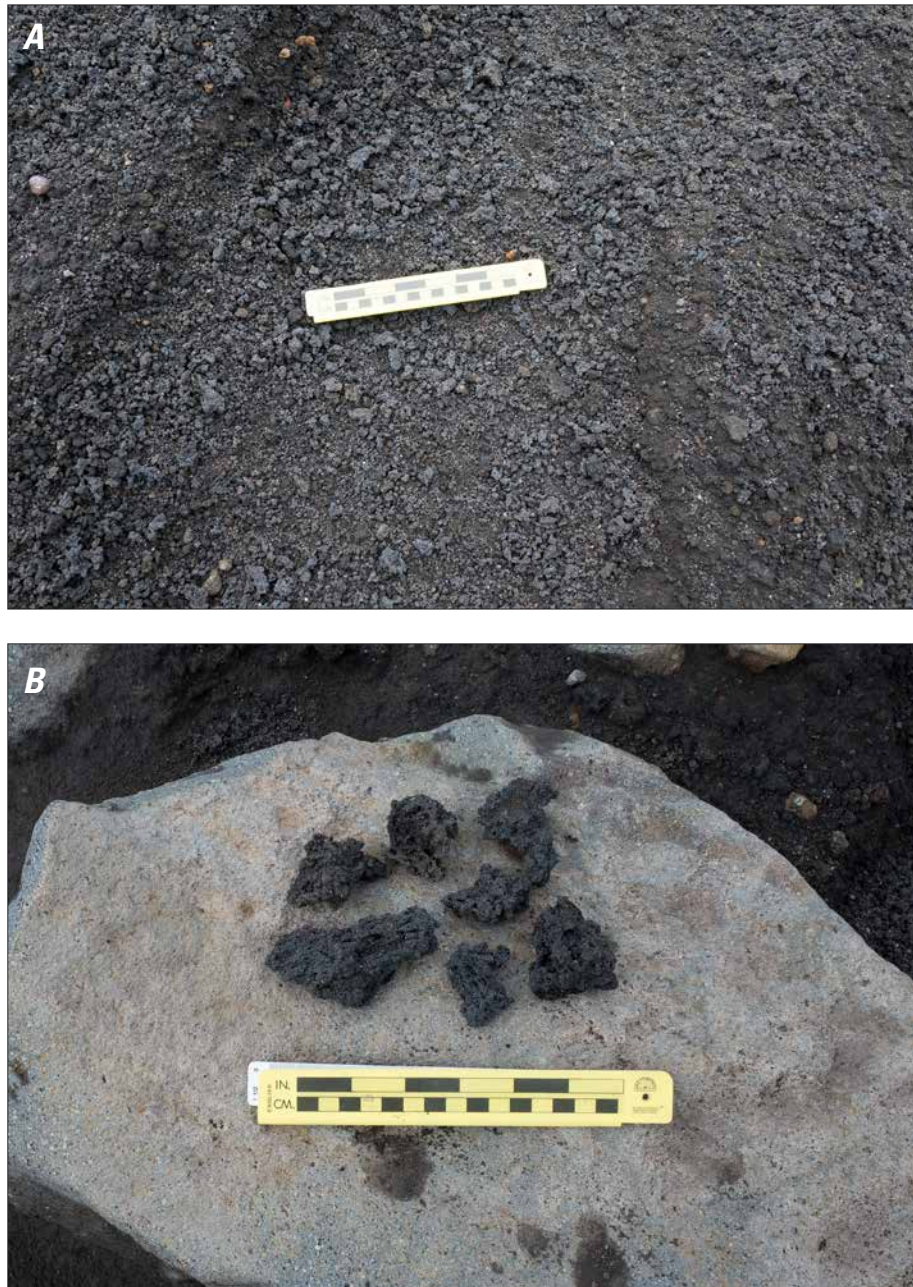


**Figure 25.** Photographs showing reworked scoriaceous lapilli lag on the surface near seismic station PN7A (fig. 1). *A*, Fines-depleted scoriaceous lapilli. Scale is 15 cm long. *B*, Representative clasts of scoria from deposit shown in *A*. Scale is 15 cm long.

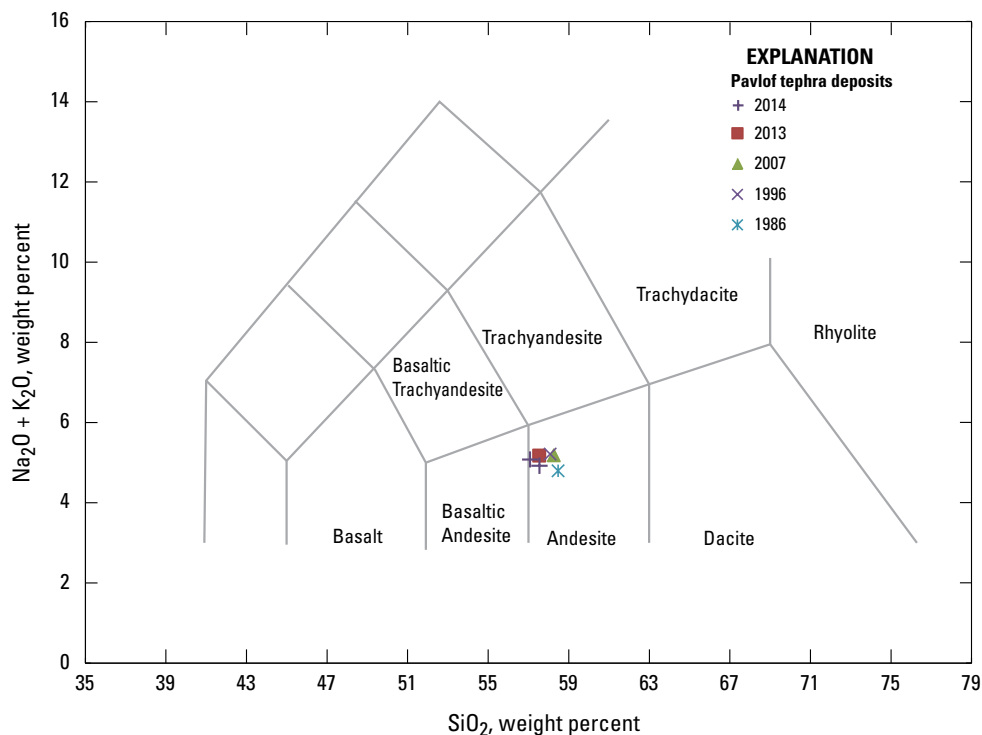


**Figure 26.** Total alkali versus silica plot for glass analyses of representative samples of tephra from recent historical Pavlof eruptions. Averaged normalized glass composition shown in appendix 2a and raw and normalized point data are in appendix 2b.

service was also suspended during this time, affecting air travel to King Cove and False Pass.

The disruption of air travel to Cold Bay and Dutch Harbor because of ash clouds from Pavlof during the 2014 eruption adversely affected the fishing industry for several days in June, members of the seafood industry workforce were unable to reach destinations in Alaska. We are unaware of any flight cancellations or disruptions during the November activity.

The drainages on the north flank of the volcano were inundated by lahars and the active channels were temporarily choked with sediment, rock debris, and boulders. The extent of inundation was relatively minor and individual flows traveled only 5–10 km beyond the base of the volcano.

## Discussion and Summary

The 2014 eruptions of Pavlof Volcano were characterized by two temporally distinct phases of eruptive activity occurring in May–June and November, separated by an intervening quiet period, when the volcano returned to its normal background state and showed no evidence of continued unrest. Therefore, each phase of the 2014 eruptive activity should be considered a separate eruptive period. The May–June eruptive period lasted 18 days and the November eruptive period last only 5 days, which makes these eruptions among the shortest duration Pavlof Volcano events documented (table 1; fig. 27). Slightly more than half of

the eruptive events since 1973 (54 percent) have had durations of 20 days or less and about 77 percent of the eruptive events lasted less than 30 days (fig. 28). Of the 35 eruptions documented since the volcano was seismically instrumented in the early 1970's (table 1), the 1974–75 (about 123 days), 1986 (104 days), and 1996–97 (111 days) eruptions are notably anomalous in terms of their respective durations (fig. 27). It is unlikely that the volcano was in a state of continuous eruption during these eruptive periods, and unfortunately there are limited observations available to help constrain the timing of individual eruptive bursts. The eruptive durations given in table 1 should be understood as the length of a given eruptive period and not a period of continuous eruption. In spite of the short duration of their eruptive activity, both the May–June and November eruptions generated relatively large fountain-fed lava flows on the northwest flank of the volcano, among the largest lava flows produced from eruptive activity at Pavlof.

Using all of the eruptive periods since 1973 that are described in table 1, the average eruption duration is 24 days and the median duration is 14 days. If the three anomalously long eruptive periods are omitted, the average eruption duration is 15 days. There appears to be no correlation between the length of an eruptive period and the length of the preceding repose period (fig. 29). Typical Pavlof eruptions show variable eruptive styles and range from sustained periods of lava fountaining to periods of violent Strombolian activity often accompanied by sustained ash emission. Ash clouds have reached as high as 11 km above sea level and extended several hundred kilometers beyond

20 The 2014 Eruptions of Pavlof Volcano, Alaska

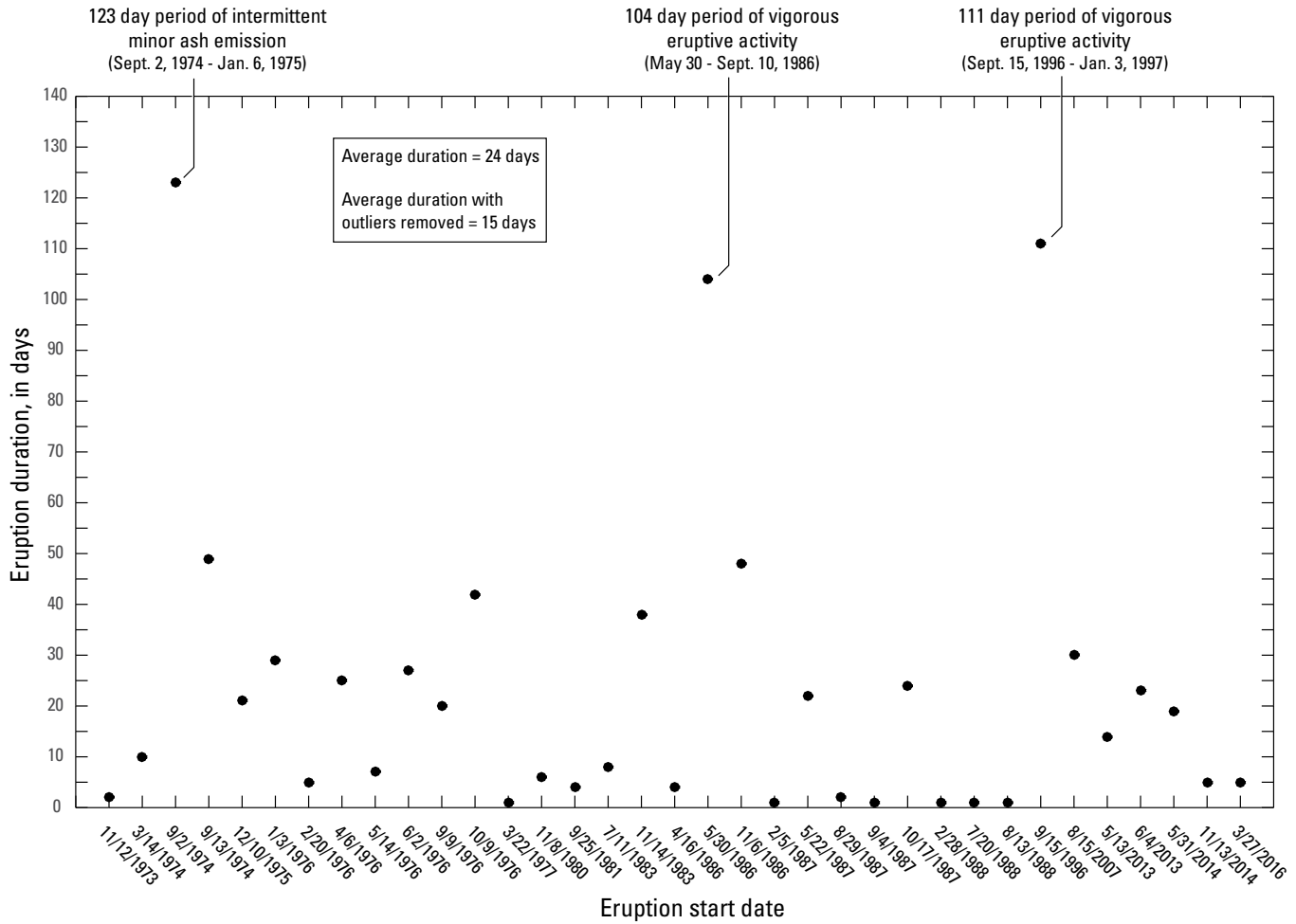


**Figure 27.** Graph of Pavlof Volcano eruption duration in days versus eruption start date. Median eruption duration is 14 days and average eruption duration is ~24 days, biased by three anomalously long duration eruptions in 1974–75, 1986, and 1996–97. If these eruptions are omitted from dataset, average eruption duration for the period 1973–2016 is 15 days. Data used to generate this plot are listed in table 1.

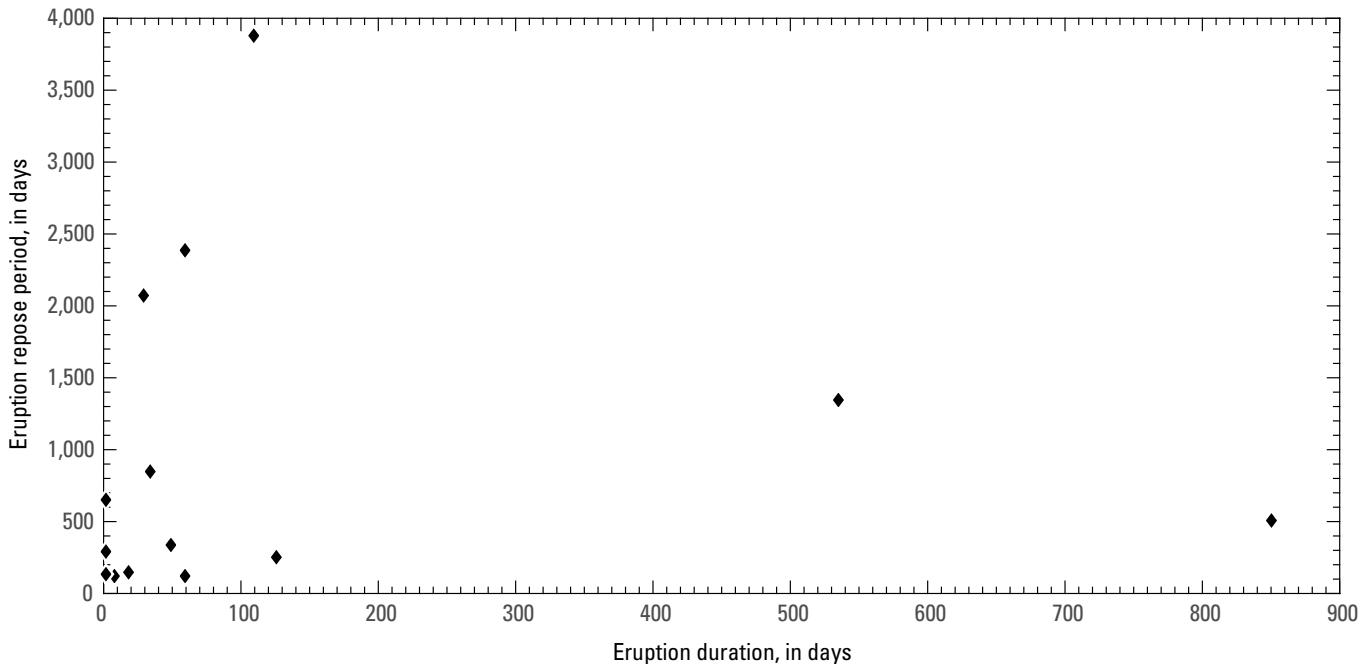


**Figure 28.** Frequency histogram of Pavlof Volcano eruption duration, 1973–2016; ~ 77 percent of the eruptions during this period lasted 30 days or less.

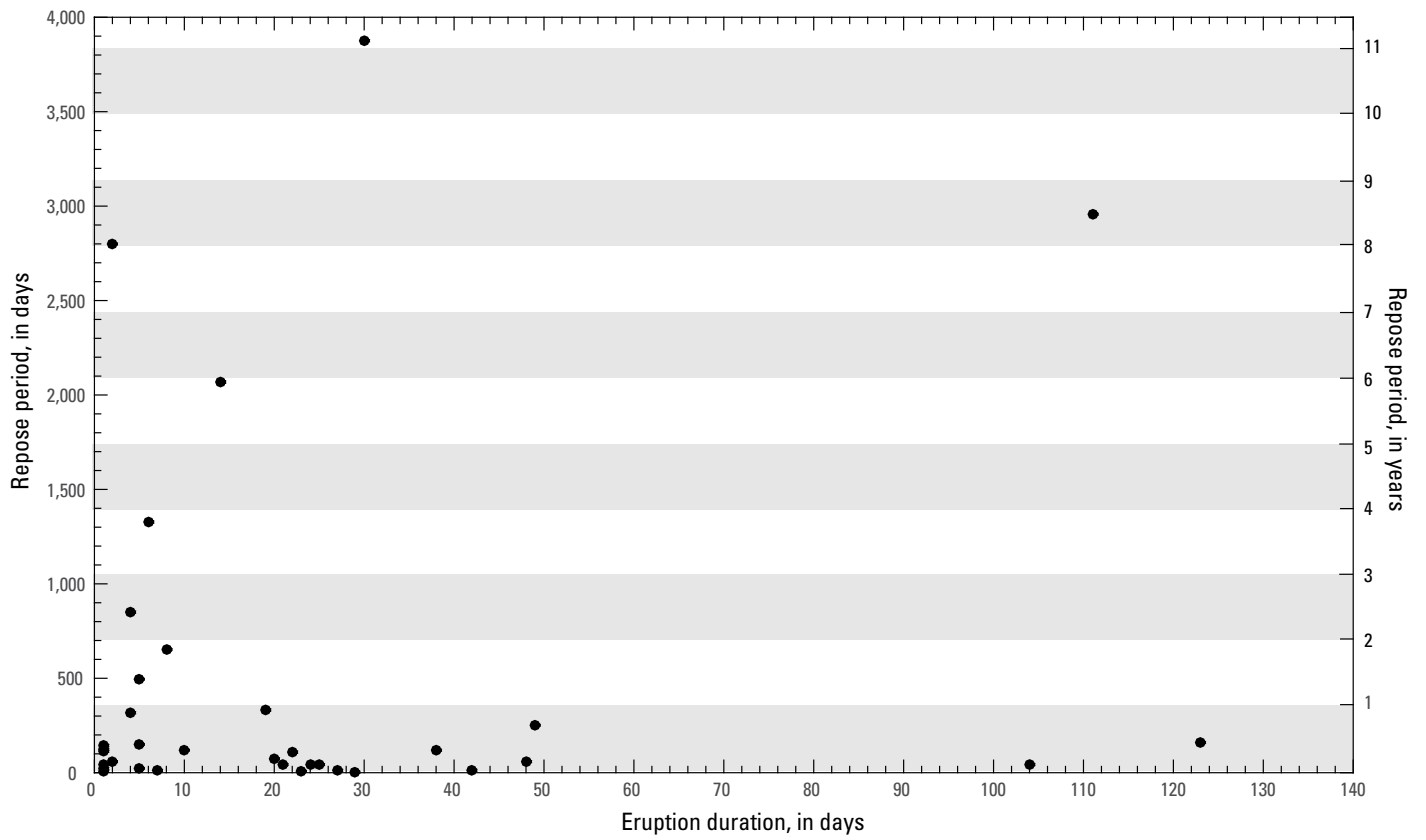


**Figure 29.** Graph of length of preceding repose period and eruption duration at Pavlof Volcano, 1973–2016.

**Table 1.** Comparison of Pavlof Volcano eruptions, 1973–2016.

[#, Start date uncertain or approximate; \*, Stop date uncertain or approximate; ?, Observation uncertain.]

Start date	Stop date	Duration of eruptive period (days)	Repose period (days)	Type of activity							Flank affected	Reference	
				Lava fountaining	Explosions	Ash emission & max. plume height (m. asl)	Fountain-fed lava flows	Hot granular mass flows	Lahars	Other			
Mar. 27, 2016	Mar. 31, 2016	5	497	X	X	X	X	X	X	X	Lightning	Northwest	Alaska Volcano Observatory (unpub. Data, 2016)
Nov. 13, 2014	Nov. 17, 2014	5	149	X	X	X (11,300)	X	X	X	X	Lightning	Southeast	This report
May 31, 2014	June 18, 2014	19	335	X	X	X (11,500)	X	X	X	X	Lightning	Northwest	This report
June 4, 2013	June 27, 2013	23	8	X	X	X (7,300)	X	X	X	X			Waythomas and others, 2014
May 13, 2013	May 27, 2013	14	2,069	X	X	X (8,500)	X	X	X	X		Northwest	Waythomas and others, 2014
Aug. 15, 2007	Sept. 13, 2007	30	3,877	X	X	X (7,000)	X	X	X	X	Lightning	Southeast	Waythomas and others, 2008; McGimsey and others, 2011
Sept. 15, 1996	Jan. 3, 1997*	111	2,956	X	X	X (9,100)	X	X	X	X	Incandescent Ejecta and intermittent activity	Northwest Northeast	Global Volcanism Program, 1996
Aug. 13, 1988#	Aug. 13, 1988*	1	25			X						All	Global Volcanism Program, 1988
July 20, 1988#	July 20, 1988*	1	144			X						North	Global Volcanism Program, 1988
Feb. 28, 1988#	Feb. 28, 1988*	1	112			X (3,100)						Northeast	Global Volcanism Program, 1988
Oct. 17, 1987	Nov. 9, 1987	24	44	X	X	X (5,800)	X	X	X	X	Pulsatory ash Emissions	Northwest, Northeast	Global Volcanism Program, 1987
Sept. 4, 1987#	Sept. 4, 1987*	1	6			X						All	Global Volcanism Program, 1987
Aug. 29, 1987#	Aug. 30, 1987*	2	59	X	X	X		X	X	X		Southeast	Global Volcanism Program, 1987
May 22, 1987#	June 12, 1987*	22	107	X	X	X (3,100)	X	X	X	X	Pulsatory ash Emissions	Northeast	Global Volcanism Program, 1987
Feb. 5, 1987	Feb. 5, 1987*	1	45			X					Possible, not confirmed	Northwest	Global Volcanism Program, 1987
Nov. 6, 1986	Dec. 23, 1986	48	58	X	X	X (5,400)	X	X	X	X	Pulsatory ash Emissions occurring intermittently	Southeast, Northwest	Global Volcanism Program, 1986
May 30, 1986	Sept. 10, 1986*	104	42	X	X	X (5,500)	X	X	X	X	Pulsatory ash Emissions occurring intermittently	East-Southeast, Northwest	Global Volcanism Program, 1986

Table 1.—Continued

Start date	Stop date	Duration of eruptive period (days)	Repose period (days)	Type of activity							Other	Flank affected	Reference
				Lava fountaining	Explosions	Ash emission & max. plume height (m, asl)	Fountain-fed lava flows	Hot granular mass flows	Lahars				
Apr. 16, 1986	Apr. 19, 1986*	4	848			X	(16,000)			X		Northwest	Global Volcanism Program, 1986
Nov. 14, 1983	Dec. 21, 1983	38	120	X	X	X	(7,500)				Chugging	Not known	Global Volcanism Program, 1983, 1984
July 11, 1983	July 18, 1983	8	652		X	X	X					Not known	Global Volcanism Program, 1983
Sept. 25, 1981	Sept. 28, 1981*	4	317	X		X	(10,500)	Possible, not confirmed	X	Possible, not confirmed		Northwest	Global Volcanism Program, 1981
Nov. 8, 1980	Nov. 13, 1980	6	1,328	X	X	X	X	X	X	X	Ballistic ejecta	Northeast, North	Global Volcanism Program, 1980
Mar. 22, 1977	Mar. 22, 1977	1	124			X	(11,000)				Minor ash emission	Summit	Global Volcanism Program, 1977
Oct. 9, 1976	Nov. 19, 1976	42	12			X	X				Steam plumes, minor ash emission	All	Global Volcanism Program, 1976
Sept. 9, 1976	Sept. 28, 1976*	20	74			X	X				Steam plumes, minor ash emission	All	Global Volcanism Program, 1976
June 2, 1976	June 28, 1976	27	14			X	(2,500)				Steam plumes, minor ash emission	All	Global Volcanism Program, 1976
May 14, 1976	May 20, 1976	7	15			X	(3,000)				Steam plumes, minor ash emission	All	Global Volcanism Program, 1976
Apr. 6, 1976 <sup>#</sup>	Apr. 30, 1976*	25	43			X	X				Steam plumes, minor ash emission	All	Global Volcanism Program, 1976
Feb. 20, 1976	Feb. 24, 1976	5	21	X		X	(3,000)		X			Northwest	Global Volcanism Program, 1976
Jan. 3, 1976	Jan. 31, 1976*	29	5	X		X	X				Steam plumes	Not reported, likely northwest	Global Volcanism Program, 1976
Dec. 10, 1975 <sup>#</sup>	Dec. 30, 1975*	21	41	X		X	X	Possible, not confirmed	X	Possible, not confirmed	Steam plumes, pulsatory emissions, chugging	Northwest	Global Volcanism Program, 1975; Shackleford, 1977
Sept. 13, 1975 <sup>#</sup>	Oct. 31, 1975*	49	250	Possible, not confirmed		X	(2,400)	Possible, not confirmed	X	Possible, not confirmed	Chugging, weak ash emission	North	Global Volcanism Program, 1975

Table 1.—Continued

Start date	Stop date	Duration of eruptive period (days)	Repose period (days)	Type of activity							Flank affected	Reference	
				Lava fountaining	Explosions	Ash emission & max. plume height (m. asl)	Fountain-fed lava flows	Hot granular mass flows	Lahars	Other			
Sept. 2, 1974	Jan. 6, 1975	123	162		X	X	Possible, not confirmed				Intermittent ash emissions of uncertain duration. Activity not continuous.	Not known	Jacob and Hauksson (1983); McNutt, 1987
Mar. 14, 1974 <sup>#</sup>	Mar. 24, 1974*	10	121			X					Minor ash emissions		Jacob and Hauksson (1983)
Nov. 12, 1973	Nov. 13, 1973	2		X			X(?)					Northwest	Stone and Kientle, 1975; McNutt, 1987

**Table 2.** Reports of ash fall on communities near Pavlof Volcano, 1846-2016.

Eruptive period or date of report	Community	Comments	Reference
March 27 to March 31, 2016	Nelson Lagoon Port Heiden	2–3 cm of coarse ash fall on Nelson Lagoon, March 27–28. Trace ash fall on Port Heiden, March 28–29	Alaska Volcano Observatory, unpub. Data, 2016
May 31 to June 18, 2014	Sand Point	Trace amounts of ash fall reported at Sand Point on June 3–4	This report; Cameron and others, 2017
May 13 to July 1, 2013	Sand Point Nelson Lagoon King Cove Cold Bay	Trace amounts of ash fall reported at a camp about 80 km northeast of Pavlof on May 14, at Sand Point, May 18–19, at Nelson Lagoon, May 19–20, at Cold Bay, June 7 and at King Cove, June 24.	Waythomas and others, 2014
Sept. 15, 1996 to Jan. 3, 1997	Nelson Lagoon	“Light” ash fall reported at Nelson Lagoon, October 28, 1996	Global Volcanism Program, 1996
Oct. 17 to Nov. 9, 1987	Canoe Bay	Unknown amount of coarse ash fall reported on October 19, 1987 at Canoe Bay, about 45 km northeast of Pavlof.	Global Volcanism Program, 1987
April 16-18, 1986	Cold Bay King Cove	About 2–3 mm of ash fall on Cold Bay and King Cove on April 16–18, 1986	McNutt and others, 1991
Sept. 25-27, 1981	Pavlof Bay	Up to 4 cm of ash fall reported on a fishing boat in Pavlof Bay, about 20 km northeast of Pavlof Volcano	Global Volcanism Program, 1981
Sept. 9-28, 1976	Sand Point	“Light” ash fall reported on Sept. 9, 1976.	Jacob and Hauksson, 1983
Nov. 12-13, 1973	Cold Bay	Ash fall on Cold Bay, amount not reported.	McNutt, 1987
October, 1917	King Cove	Trace ash fall on King Cove reported during an unspecified eruption, October 1917	Jaggard, 1929
July 6, 1914	Unga Island	Ash fall on Unga Island reported on July 6, 1914, amount not reported	Kennedy and Waldron, 1955 Jaggard, 1929
August 15, 1846	Pavlof village Unga Island	Ash fall reported on the now abandoned village of Pavlof on the east shore of Pavlof Bay about 25 km east of Pavlof. Ash fall also reported on Unga Island about 70 km southeast of Pavlof. Amounts of ash fall not reported.	Kisslinger, 1983

the volcano. Lahar inundation of the drainages on the volcano depends on the amount of meltwater produced from ice and snow, which is primarily related to the frequency of hot granular avalanches caused by collapse of spatter accumulations on the upper flank of the volcano. Fountain-fed lava flows also generated meltwater where they encounter snow and ice, but the melt rates are significantly lower than those associated with hot granular avalanches and any resulting lahars are small in volume.

## References Cited

- Cameron, C.E., Dixon, J.P., Neal, C.A., Waythomas, C.F., Schaefer, J.R., and McGimsey, R.G., 2017, 2014 Volcanic activity in Alaska—Summary of events and response of the Alaska Volcano Observatory: U.S. Geological Survey Scientific Investigations Report 2017-5077, 81 p., <https://doi.org/10.3133/sir20175077>.
- Cas, R.A.F., and Wright, J.V., 1987, Volcanic successions modern and ancient—A geological approach to processes, products and successions: New York, Chapman & Hall, 528 p.
- De Angelis, S., Fee, D., Haney, M., and Schneider, D., 2012, Detecting hidden volcanic explosions from Mt. Cleveland Volcano, Alaska with infrasound and ground-coupled airwaves: *Geophysical Research Letters*, v. 39, no. 21, at <https://doi.org/10.1029/2012GL053635>.
- Fee, D., Haney, M., Matoza, R., Szuberla, C., Lyons, J., and Waythomas, C.F., 2016, Seismic envelope-based detection and location of ground-coupled airwaves from volcanoes in Alaska: *Bulletin of the Seismological Society of America*, v. 106, no. 2, p. 1024–1035.
- Global Volcanism Program, 1975, Report on Pavlof (United States), in Squires, D., ed., *Natural Science Event Bulletin*: Smithsonian Institution, v. 1, no.1, at <http://dx.doi.org/10.5479/si.GVP.NSEB197510-312030>.

- Global Volcanism Program, 1976, Report on Pavlof (United States), *in* Squires, D., ed., *Natural Science Event Bulletin: Smithsonian Institution*, v. 1, no. 4, at <http://dx.doi.org/10.5479/si.GVP.NSEB197601-312030>.
- Global Volcanism Program, 1977, Report on Pavlof (United States), *in* Squires, D., ed., *Natural Science Event Bulletin: Smithsonian Institution*, v. 2, no. 4, at <http://dx.doi.org/10.5479/si.GVP.NSEB197704-312030>.
- Global Volcanism Program, 1980, Report on Pavlof (United States), *in* Squires, D., ed., *Scientific Event Alert Network Bulletin: Smithsonian Institution*, v. 5, no. 11, at <http://dx.doi.org/10.5479/si.GVP.SEAN198011-312030>.
- Global Volcanism Program, 1981, Report on Pavlof (United States), *in* McClelland, L., ed., *Scientific Event Alert Network Bulletin: Smithsonian Institution*, v. 6, no. 9, at <http://dx.doi.org/10.5479/si.GVP.SEAN198109-312030>.
- Global Volcanism Program, 1983, Report on Pavlof (United States), *in* McClelland, L., ed., *Scientific Event Alert Network Bulletin: Smithsonian Institution*, v. 8, no. 11, at <http://dx.doi.org/10.5479/si.GVP.SEAN198311-312030>.
- Global Volcanism Program, 1984, Report on Pavlof (United States), *in* McClelland, L., ed., *Scientific Event Alert Network Bulletin: Smithsonian Institution*, v. 9, no. 1, at <http://dx.doi.org/10.5479/si.GVP.SEAN198401-312030>.
- Global Volcanism Program, 1986, Report on Pavlof (United States), *in* McClelland, L., ed., *Scientific Event Alert Network Bulletin: Smithsonian Institution*, v. 11, no. 3, at <http://dx.doi.org/10.5479/si.GVP.SEAN198603-312030>.
- Global Volcanism Program, 1987, Report on Pavlof (United States), *in* McClelland, L., ed., *Scientific Event Alert Network Bulletin: Smithsonian Institution*, v. 12, no. 3, at <http://dx.doi.org/10.5479/si.GVP.SEAN198703-312030>.
- Global Volcanism Program, 1988, Report on Pavlof (United States), *in* McClelland, L., ed., *Scientific Event Alert Network Bulletin: Smithsonian Institution*, v. 13, no. 7, at <http://dx.doi.org/10.5479/si.GVP.SEAN198807-312030>.
- Global Volcanism Program, 1996, Report on Pavlof (United States), *in* Wunderman, R., ed., *Bulletin of the Global Volcanism Network: 21:12. Smithsonian Institution*, v. 21, no. 12, at <http://dx.doi.org/10.5479/si.GVP.BGVN199612-312030>.
- Mangan, M.M., Miller, T.P., Waythomas, C.F., Trusdell, F., Calvert, A.T., and Layer, P.W., 2009, Diverse lavas from closely spaced volcanoes drawing from a common parent—Emmons Lake Volcanic Center, Eastern Aleutian Arc: *Earth and Planetary Science Letters*, v. 287, p. 363–372, at <https://doi.org/10.1016/j.epsl.2009.08.018>.
- McGimsey, R.G., Neal, C.A., Dixon, J.P., Malik, N., and Chibisova, M., 2011, 2007 Volcanic activity in Alaska, Kamchatka, and the Kurile Islands—Summary of events and response of the Alaska Volcano Observatory: U.S. Geological Survey Scientific Investigations Report 2010-5242, 110 p., at <http://pubs.usgs.gov/sir/2010/5242/>.
- McNutt, S.R., 1987, Eruption characteristics and cycles at Pavlof Volcano, Alaska, and their relation to regional earthquake activity: *Journal of Volcanology and Geothermal Research*, v. 31, no. 3–4, p. 239–267.
- McNutt, S.R., Miller, T.P., and Taber, J.J., 1991, Geological and seismological evidence of increased explosivity during the 1986 eruptions of Pavlof Volcano, Alaska: *Bulletin of Volcanology*, v. 53, no. 2, p. 86–98.
- Miller, T.P., Neal, C.A., and Waitt, R.B., 1995, Pyroclastic flows of the 1992 Crater Peak eruptions— Distribution and origin, *in* Keith, T. E. C., ed., *The 1992 eruptions of Crater Peak vent, Mount Spurr Volcano, Alaska: U.S. Geological Survey Bulletin 2139*, p. 81–87.
- Roach, A.L., Benoit, J.P., Dean, K.G., and McNutt, S.R., 2001, The combined use of satellite and seismic monitoring during the 1996 eruption of Pavlof volcano, Alaska: *Bulletin of Volcanology*, v. 62, no. 6, p. 385–399.
- Shackelford, D. C., 1977, Pavlof, *in* *Annual report of the world volcanic eruptions in 1975 with supplements to the previous issues: Bulletin of Volcanic Eruptions*, v. 15, p. 41.
- Sumner, J.M., 1998, Formation of clastogenic lava flows during fissure eruption and scoria cone collapse—The 1986 eruption of Izu-Oshima Volcano, eastern Japan: *Bulletin of Volcanology*, v. 60, no. 3, p. 195–212.
- Waythomas, C.F., Haney, M.M., Fee, D., Schneider, D.J., and Wech, A., 2014, The 2013 eruption of Pavlof Volcano, Alaska—A spatter eruption at an ice- and snow-clad volcano: *Bulletin of Volcanology*, v. 76, no. 10, p. 862, at <https://doi.org/10.1007/s00445-014-0862-2>.
- Waythomas, C.F., Prejean, S.G., and McNutt, S.R., 2008, Alaska’s Pavlof Volcano ends 11-year repose: *Eos*, v. 89, no. 23, p. 209–21.

# Appendixes 1–2

[Available for download at <https://doi.org/10.3133/sir20175129>]

Appendix 1. Chemical data for The 2014 Eruptions of Pavlof Volcano.

Appendix 2a. Major-oxide glass geochemistry for historical Pavlof tephra fall deposits.

Appendix 2b. Point and normalized major-element glass compositions from select tephra falls from Pavlof volcano, determined by electron probe microanalyzer at the U.S. Geological Survey in Menlo Park, California.

